Postsynaptic Maturation of Excitatory Synapses

by

Kenneth Ray Tovar

A DISSERTATION

Presented to the Graduate Program in Neuroscience

and the Oregon Health Science University

School of Medicine

in partial fulfillment of

Doctor of Philosophy

November 2000.

School of Medicine
Oregon Health Sciences University

CERTIFICATE OF APPROVAL

This is to certify that the Ph.D. thesis of
Ken Tover
has been approved

[redacted]
Committee Chair

[redacted]
Member

[redacted]
Member

[redacted]
Member

[redacted]
Member

Member

Associate Dean for Graduate Studies

TABLE OF CONTENTS

Acknowledgments

It's unclear from where a thesis arises, and perhaps especially this one. The ingredients that compose it result from much more than the work that makes up its parts. In this way, the aid that was offered and given in its construction must also result from many sources. For constant love and support through more years of school than I would care to recount I thank my mother, Mary Mendoza. Additionally, I thank those people who are dear to me and who were or became close to me throughout my graduate school stint. These include Crista Barberini, Rich Clark, Peter Edwards, Kirsten Jensen, Indira Raman and Noel Ruiz. Thank you for your presence during these years and may you never have to listen to me complain again. I also thank fellow lab members Johannes Krupp, Matt Jones, Linda Overstreet and Nathan Schoppa for their invaluable discussions about all manner of things and almost daily help. I thank all those who ever read an manuscript of mine or allowed me to bother them in their office with questions or fanciful ideas for experiments. I hope you know who you are. Jeff Volk, Kathleen Sprouffske and Ashleigh Miller were technicians who actually did the work that made it easier for me to do experiments and I so greatly appreciate that to this day. For reagents and animals I thank Drs. Jim Boulter, Stephen Heinemann, Masayoshi Mishina, Shigetada Nakanishi and Bryce Vissel. Major parts of this work were supported by the National Institutes of Mental Health (MH11204) and the Scottish Rite Schizophrenia Research Program, N.M.J., U.S.A. I gratefully acknowledge them for their funding.

The relationship between advisor and advisee is similar to an arranged marriage. The principals are largely unknown to each other and each hopes they will get what they want out of the relationship. When I barged into Gary Westbrook's office one afternoon and requested to work in his lab he knew nothing about me yet agreed to admit me to his lab. Gary provided a rich and generous work environment and showed patience and willingness to allow my work to travel outside the scope of the lab. Hopefully I did not take too much advantage of that, and instead took advantage of the proximity of his extraordinary scientific mind and ability to communicate scientific ideas. Gary's scientific rigor and creativity will be the standard to which I will hold my own work. I thank him for imparting these things on me.

Abstract

The goal of my work was to investigate the initial events of synapse formation following *N*-methyl-D-aspartate (NMDA) receptor insertion into the postsynaptic membrane. Using cultured rat and mouse hippocampal neurons in microculture, we investigated the cellular patterns of expression of the ε1 and ε2 NMDA receptor subunits (NR2A and NR2B in rats) that together with the ζ1 subunit (NR1 in rats) combine to form NMDA receptors. We did this physiologically, combining whole-cell voltage clamp recording with the use of subunit-specific antagonists. When neurons are plated in a microculture system, they form synapses on themselves, or autapses. This allowed us to record from the soma of a neuron that is its own pre- and postsynaptic cell. Using this system, we found a subunit-dependent differential targeting of receptors to synaptic and extrasynaptic membrane. As synapses on individual neurons matured NMDA receptors with two distinct subunit compositions are expressed within that neuron's synaptic complement. We used targeted mutant mice that lacked either ε1, ε2 or both to we verify the expression patterns of these subunits and study the behavior of synapses. Excitatory postsynaptic currents (EPSCs) from $\varepsilon 2^{-/-}$ neurons had currents consistent with expression of ζ1/ε1 receptors while neurons from $\varepsilon 1^{-/-}$ mice had currents consistent with the expression of ζ1/ε2 receptors. Neurons lacking both subunits lacked functional NMDA receptors but formed synapses normally. Finally, we present evidence that a significant fraction of the NMDA receptors that respond to synaptically-released glutamate are not fixed at synapses. This implies that the early structure of the synapse is not as rigid as previously thought and runs counter to the notion that neurotransmitter receptors must be tightly fixed immediately beneath the site of transmitter release. This work provides a starting point for understanding the development of synapses in the central nervous system.

Introduction

One view of central synapse formation and maturation

A self-organizing system is one that forms and changes as a function of its experience or environment. During development, many regions of the vertebrate central nervous system (CNS) exhibit properties of self-organizing systems. This fact was initially appreciated in the 1950s by Hubel and Weisel. Their studies on the visual system of cats and primates (Hubel and Weisel, 1998) were among the first examples of self-organization in the developing nervous system. By creating input disparities between the eyes in binocular animals, they were able to manipulate the extent of visual cortex that was innervated by inputs from each eye. While the developing visual system has been the most extensively studied, self-organization is evident in several other portions of the cortex, as well as in many subcortical regions. The basic experimental phenomenology that activity drives development, initially demonstrated in the visual system, has been replicated in other areas, including the somatosensory and auditory systems (Fox et al., 2000; Doupe and Solis, 1997). It is largely from this long history of work that the concept of 'activity-dependence' in developmental processes has arisen.

The development of the nervous system through self-organization and guided by activity, is thought to occur via spontaneous patterned activity or on sensory activation of incipient neural networks. For example, bursts of spontaneous action potential in the retina are thought to be involved in the patterning of inputs in the thalamic lateral geniculate nucleus (Wong, 1999; Wong and Oakley, 1996) while the extent of thalamic inputs to the cortex can be altered by blockade of activity (Kleinschmidt et al., 1987). These self-organizational processes operate through incipient neural networks, and thus across synapses that are already present in the network. As a result of activity in incipient networks, the cortex and subcortical regions undergo large-scale changes in their presynaptic inputs. This implies that new synapses may form as a result of activity-dependent rearrangement of inputs. However, it seems equally likely that synapses are also being eliminated (Chen and Regehr, 2000). Specifically, those synapses that were somehow deemed inappropriate are removed while new synapses form. Therefore, one

way of asking the same question that systems physiologists have asked about self-organizing systems is to ask, "How does activity act at synapses during activity-dependent synaptic rearrangement?"

Because of the important role of information transfer across nascent synapses, if we are to understand the rules by which the cortex develops, we must understand not only the behavior of nascent synapses but also what characterizes a nascent synapse and whether it is these characteristics that enable a synapse to undergo activity-dependent changes in stability or efficacy. From an understanding of the rules by which synapses are formed, maintained and eliminated can emerge a bottom-up approach to cortical self-assembly. A set of these characteristics would reveal the constraints on models of 'activity-dependent' processes in cortical circuit maturation. By understanding the locus of activity at the cellular and synaptic level and its effect on individual synapses, a list of rules should emerge for what must occur epigenetically as multiple inputs become organized during cortical maturation.

Synapses and synaptic development

The amino acid glutamate is the predominant excitatory neurotransmitter in the vertebrate CNS. At fast excitatory synapses, there are two predominant types of ligand-gated ion channel receptors that respond to glutamate, α-amino-3-hydroxy-5-methyl-4-isoxazole-proprionic acid (AMPA) receptors and *N*-methyl-D-aspartate (NMDA) receptors. Until recently, it was thought that these receptors were colocalized at most excitatory synapses (Bekkers and Stevens, 1989; Jones and Baughman, 1990). At resting membrane potentials, colocalization of AMPA and NMDA receptors can be required for significant ion flux through NMDA receptor channels that are blocked in a voltage-dependent manner by magnesium (Mayer et al., 1984, Nowak et al., 1984). At synapses with both receptor types, magnesium block can be relieved by the gating of AMPA receptors and subsequent local depolarization. Because of the voltage-dependence of the NMDA channel, to a first approximation, synapses that contain only NMDA receptors are functionally silent. The recent interest in silent synapses has perhaps given the impression that they are more prevalent. While many synapses can contain only NMDA

receptors, these synapses appear to be in the minority (Bekkers and Stevens, 1989; Jones and Baughman, 1990). While the incidence of silent synapses may be initially relatively high and decreases with development, they still appear to be in the minority (Isaac et al., 1997; Chen and Regehr, 2000). The number of these synapses may, however, not necessarily be linked to their physiological importance.

The vertebrate neuromuscular junction (NMJ) is the most thoroughly studied fast chemical synapse. It was at the NMJ where fast chemical transmission was definitively demonstrated (Dale et al., 1936), where the cellular physiology of synapses was first probed and the quantal nature of synaptic transmission was revealed (see Katz, 1963). The extent of the work on the NMJ provides the foundation for the study of central synapses. Additionally, the NMJ provides a set of expectations from which we can make initial assumptions about the behavior of other fast chemical synapses. The generalization regarding the NMJ also holds true for the study of its development.

What is required for synapse formation to occur? Prior to synapse formation in the NMJ, the three cell types that participate in the process (nerve, muscle cell and Schwann cell) are largely differentiated (Sanes and Lichtman, 1999). By analogy, neurons seem to possess characteristics typical of pre- and postsynaptic membranes prior to synapse formation (Fletcher et al., 1994). Thus, as a first step it seems that neuronal cell membranes need to be differentiated with respect to their final destiny, i.e. pre- and postsynaptic. A minimal list of required elements for a functional presynaptic terminal includes presynaptic vesicles, neurotransmitter synthesis and vesicle loading enzymes, neurotransmitter release machinery and associated Ca^{++} channels and the proteins to hold everything in place at the appropriate density. This list does not include sodium and potassium channels required for initiation, conduction and timing of action potentials. On the postsynaptic side there needs to be the appropriate receptors for the neurotransmitter released, and the proteins that hold a physiologically relevant density of receptors in apposition to sites of neurotransmitter release.

To initiate synaptic transmission following pre- and postsynaptic membrane differentiation, some form of recognition and signaling must take place between the two adjacent membranes. There are several possible ways for this to occur. The presynaptic terminal could

find a differentiated postsynaptic membrane, with receptors clustered at the appropriate density for effective signaling or the postsynaptic membrane must be capable of specialization in response to presynaptic clustering signals. The latter possibility appears to occur at the NMJ because new clusters of acetylcholine receptors (AChRs) appear when pre- and postsynaptic membranes contact, even though AChR accumulations are seen prior to synapse formation (Frank and Fischbach, 1979). Motoneurons do not appear to seek out preformed AChR clusters. Moreover, AChR clusters subjacent to the ingrowing motoneuron result from the direct action of neurons on muscle cell membrane (Reist et al., 1992). Additionally, the presynaptic terminal releases factors that change the expression patterns of AChR subunits (Martinou et al., 1991; Falls et al., 1993). Recent evidence indicates that small clusters of AChR can form in the end-plate band where incoming neurons are likely to initiate synapse formation (Lin et al., 2001). Whether this result indicates that the steps in reciprocal differentiation begin postsynaptically remains to be seen. Thus at the NMJ, evidence indicates that while signaling reciprocity between pre- and postsynaptic membranes occurs as a function of development, the communication between membranes appears to be initiated by the presynaptic terminal.

In central neurons, while sites containing pre- and postsynaptic markers can appear in less than an hour after initial contact by presynaptic process (Friedman et al., 2000) it is not known which membrane initiates communication. Dendritic filopodial dynamics may be important in initiating synapse formation during development in central neurons. Dendritic filopodia extend and contact axonal membrane (Ziv and Smith, 1996; Fiala et al., 1998) and may be the earliest precursors to dendritic spines. Dendritic spine motility is highly dynamic (Fischer et al., 1998) and the stability of spines can be modified by treatments that affect synaptic transmission. In one recent study, actin motility in spines was inhibited by AMPA or NMDA receptor activation (Fischer et al., 2000). In contrast, the rate of movement of dendrites in the retinal was greatly inhibited by treatment with AMPA or NMDA receptor antagonists (Wong et al., 2000). However, the relationship of dendritic spine motility to synapse formation is not known.

Unlike the case at the NMJ (Gautam et al., 1996), in central neurons, there are no known manipulations that prevents synapse formation. At the NMJ, while the AChR (and thus AChR

function) is not required for formation of the synapse (Westerfield et al., 1990), events that could be referred to as maturational are dependent on functional AChRs (Fischbach et al., 1979). Similarly, in central neurons, block of synaptic transmission does not prevent synapse formation (Segal and Furshpan 1990; Rao and Craig, 1998). However, activity may affect synaptic maturation. Postsynaptic sites that contain only NMDA receptors have been implicated in long-term potentiation (LTP; Isaac et al., 1995; Liao et al., 1995). The incidence of 'silent synapses' appears to decrease with development (Durand et al., 1996; Wu et al., 1996; Isaac et al., 1997), indicating that activity may be required for maturation from NMDA-only synapses to synapses that contain AMPA and NMDA receptors. Despite strong evidence to the contrary (Li et al., 1994; Cottrell et al., 2000) the inference often drawn is that there is a necessary developmental sequence from 'silent synapses' to fully functional synapses, ones that contain AMPA and NMDA receptors.

Several models of cortical development have been proposed for systems containing only NMDA receptors at synapses (Ben-Ari et al., 1997; Constantine-Paton and Cline, 1998). These models require the input of GABAergic interneurons or the regenerative action of NMDA receptor-mediated excitatory postsynaptic potentials (Sah et al., 1989). Because these theoretical constructs require depolarization of the entire neuron, possibly by synaptic inputs that ultimately would not end up being strengthened, it is unclear, how such mechanisms could operate within the constraints of the Hebbian hypothesis from which they result (Hebb, 1973). Additionally, in some systems known to undergo activity-dependent synaptic rearrangements, NMDA-only synapses appear to have no obvious role during the time when inputs are altered (Hohnke et al., 2000; Chen and Regehr, 2000).

While activity may cause synaptic maturation, it is equally likely that activity acts primarily in the elimination of inappropriate inputs. Synapse elimination has been well studied in the vertebrate NMJ (see Lichtman and Colman, 2000). Synapse elimination may also play an important role in the development of the cortex. For example, in the kitten visual cortex, when one eye is sutured, creating an activity imbalance, retraction of axonal processes of neurons from the deprived eye occurs within a few days (Antonini and Stryker 1993), a time course similar to elimination of input at the neuromuscular junction (Balice-Gordon and Lichtman, 1994). At the

NMJ, while nAChRs are not required for initial synapse formation (Westerfield et al., 1990; see Frank and Fischbach, 1979) events that could be referred to as maturational, like accumulation of acetylcholine esterase or other basal lamanina components, are affected by AChR blockade or TTX application (Fischbach et al., 1979; Sanes and Kawrence). Similarly, in central neurons, NMDA receptor activity is not required for synapse formation (Segal and Furshpan 1990; Rao and Craig, 1998). However, synaptic NMDA receptors retain characteristics of the most nascent synaptic receptors, those having relatively slow deactivation kinetics and a pharmacology consistent with NR1/NR2B subunits, which are expressed early indevelopment (Chavis and Westbrook, 2001). Thus, NMDA receptor activity may be required for events following synapse formation and may play an important role in stabilizing synapses.

It is possible that the enthusiasm generated from the study of long-term potentiation has overflowed onto other areas and that synaptic plasticity in the adult has very little, if anything, to do with synapse formation or with cortical development. It seems reasonable to consider the basic phenomenology of synapse formation in the absence of the contextual framework derived from study of synaptic plasticity. To develop reasonable models of self-assembly in the CNS, it may be important to remember that synapses form, mature and are eliminated. How we approach these questions may affect the answer. For example, are synapses stabilized or simply not eliminated? If the answer is the former, is synapse stabilization identical to maturation? If the answer is the latter, are synapses continually in danger of being eliminated and if so, what controls elimination? Does maturation preclude elimination and does maturation protect against elimination? What are the characteristics of a mature synapse?

The work in this thesis was an attempt to begin to answer questions regarding the events of excitatory synapse formation. Cultured hippocampal neurons were used throughout because cell culture neurons can be easily manipulated and because the properties of hippocampal neurons are well-known. In most instances, neurons were cultured on islands of glia which results in the formation of autaptic synapses (Bekkers and Stevens, 1991). In addition to allowing for ease of stimulation and recording of postsynaptic currents, this culture system limits inputs to the glial island. This provides control of all the synapses on a neuron in cases where a single neuron is present on an island. By taking advantage of this system where all synaptic inputs are

accounted for, we can begin to ask questions about how neurons allocate, form and eliminate synapses.

The work contained in this dissertation was done as an initial step towards addressing the problem of synapse formation in the central nervous system. As such, it is largely descriptive but hopefully provides places to begin asking questions. Chapter 1 contains a description of the molecular composition of synaptic NMDA receptors during development and demonstrates what molecular changes occur with time. We also show that there is a subunit-dependent difference in targeting of NMDA receptors. Chapter 2 uses neurons from targeted mutant mice to examine the role of the ε2 subunit early in development and targeting of the NMDA receptor. NMDA receptors with characteristics of ζ1/ε1 receptors are expressed in the absence of ε2. Chapter 3 expands this examination by using neurons from mice lacking the ε1 subunit, as well as ε1 and ε2 sununits. Cultured hippocampal neurons contain only ε1 and ε2 and do not form functional NMDA receptors when both of these are absent. In Chapter 4, we demonstrate that synaptic NMDA receptors are dynamic with respect to sites where glutamate is released. Most of the receptors can move in or out of the synapse within minutes. This reveals a potentially new way to regulate the efficacy of NMDA-receptor-mediate synaptic transmission.

The Materials and Methods are divided into sections corresponding to work from individual chapters.

Materials and Methods, Chapter 1:

Neuronal cell culture

Microisland cultures were prepared as previously described (Bekkers and Stevens, 1991). Glass coverslips (31 millimeter; Biophysica, Baltimore, MD) were placed in 35 mm culture dishes (Nunc, Denmark), coated with 0.15% agarose and allowed to dry. Using an atomizer, a solution of poly-D-lysine (0.1875 mg/ml in 17 mM acetic acid; Sigma, St. Louis, MO) and collagen (0.05 mg/ml; Collagen Corporation, Redwood City, CA) was sprayed on the agarose background to yield microdots of 100-1000 μm. After growth of glial feeder layers on the microdots, the CA1 region of hippocampi from P0-P1 rats were removed, enzymatically (papain; Collaborative Research, Bedford, MA) and mechanically dissociated and plated. Cultures were treated on day 1 with FUDR (0.2 mg/ml 5'-fluoro-2-deoxyuridine and 0.5 mg/ml uridine, Sigma) to reduce glial proliferation, and then media was exchanged weekly.

Expression of recombinant NMDA receptors

HEK293 cells were transfected 6-12 hours after plating on 31 mm coverslips. NR1-1a, NR2x and lymphocyte CD4 receptor cDNAs were transfected in a 4:4:1 ratio using the calcium phosphate method (Chen and Okayama, 1987). In cases where two different NR2 subunits were transfected, the total amount of NR2 subunit (1 μg) was kept constant (e.g. for 1:100 NR2A:NR2B, 0 .01 μg NR2A and 0.99 μg NR2B were transfected). The transfection was ended after 8-16 hours by replacing the solution with fresh media (DMEM plus 10% fetal calf serum; 1% glutamine and 1% penicillin-streptomycin, FUDR). Kynurenic acid (3 mM; Sigma) and D,L-AP5 (1 mM; Tocris, Ballwin, MO) were added to prevent glutamate-induced excitotoxicity (Cik et al., 1993). Transfected cells were identified using CD4 receptor antibody-coated beads (Dynabeads M-450 CD4; Dynal, Norway). Prior to recording, 1 μL of Dynabead suspension was added to HEK293 cells in 1 mL of media and gently rocked for 15-30 minutes. NR1-1a and NR2B cDNAs were gifts

from Jim Boulter and Stephen Heinemann (Salk Institute). NR2A cDNA was a gift from Shigetada Nakanishi (Kyoto). Bluescript cDNA encoding NR1-1a, NR2A and NR2B were inserted into pcDNA1/AMP (Invitrogen; Krupp et al., 1996). Lymphocyte CD4 receptor cDNA was inserted into the JPA vector provided by John Adelman (Vollum Institute). NR1-1a, the predominantly-expressed splice variant in the CNS (Laurie et al, 1995), was used throughout these experiments.

Whole-cell recording and solutions

Whole-cell voltage clamp recordings were performed on transfected HEK293 cells 12-72 hours after the end of the transfection reaction. Recordings from neurons were performed after 1-21 days *in vitro* (DIV). Cells were placed in a recording chamber at room temperature and continually perfused with an extracellular solution containing (in mM): NaCl (168); KCl (2.4); HEPES (10); D-glucose (10); glycine (0.001-0.01) and $CaCl_2$ (1.3). The solution pH and osmolality were adjusted to final values of 7.4 and 325 mmol/kg, respectively. To reduce calcium-dependent inactivation of NMDA receptors (Legendre et al., 1993), 0.2 mM external calcium was routinely used in agonist-containing solutions. For experiments requiring whole-cell drug applications, the intracellular solution contained (in mM): Cs-methanosulfonate (125); CsCl (15); HEPES (10); Cs_4-BAPTA (5); Na_2-ATP (2); $MgCl_2$ (3). Intracellular solution for synaptic recordings contained (in mM): K-gluconate (150); $CaCl_2$ (6.23); $MgCl_2$ (2); EGTA (10); HEPES (10); NA_2ATP (2); Na_3GTP (0.2). The pH of intracellular solutions was adjusted to 7.4 with CsOH or KOH and osmolality was adjusted to 315 mmol/kg. The pCa of this solution was calculated to be 7.0. Recording electrodes were pulled from borosilicate glass (TW150F-6; World Precision Instruments, Sarasota, FL) and had resistances between 1.5 and 5 MΩ.

For drug application experiments, the membrane voltage was usually held at -60 mV, and at -60 to -80 mV for synaptic recordings. Series resistance was always compensated (70-90%). Cell input resistances ranged from 400-1200 MΩ for HEK293 cells and 200-700 MΩ for neurons. Autaptic EPSCs were evoked by 0.5 to 2 millisecond depolarizations to 0-20 mV. The depolarization resulted in an unclamped action potential followed by an autaptic EPSC. Data were collected using an Axopatch 1C and pClamp 5 software (Axon Instruments, Foster City,

CA) acquired at a rate of 5 kHz and filtered at 0.05-2.5 kHz (eight-pole Bessel; Frequency Devices, Haverhill, MA).

NMDA (1 mM; Tocris), glutamate (1 mM; Sigma) and ifenprodil (1-10 μM; Dr. B. Scanton, Synthelabo) were dissolved in extracellular solution. Some aliquots of ifenprodil were solubilized in ethanol; final ethanol concentration was 0.025% v/v. This concentration of ethanol had no effect of whole-cell NMDA currents (data not shown). Drug applications were done using quartz flow pipes positioned 50-150 μm from the cell. Each flow pipe was controlled by a solenoid valve that, in turn, was controlled by an external timer (Winston Instruments; Palo Alto, CA). Flow pipe translations were made by an attached piezo-electric bimorph driven by a stimulus isolation unit (Winston Instruments). Neurons were equilibrated in 3 μM ifenprodil before and during agonist applications (1 mM glutamate; 100 msec duration). For synaptic recordings, neurons were equilibrated in 3 μM ifenprodil. For whole-cell experiments 300 nM tetrodotoxin (TTX; Sigma) and the AMPA receptor antagonist 6-cyano-7-nitroquinoxaline-2,3-dione (CNQX, 5 μM; Tocris) were added to the extracellular solution. TTX was omitted from synaptic experiments.

Data analysis

All data was analyzed using Axograph software (Axon Instruments). Unless otherwise specified, currents from equilibrium drug application experiments were measured using a 500-1000 msec window after currents had reached steady-state amplitude. For NMDA receptor-mediated EPSCs, currents were measured using a 5 to 10 millisecond window centered at the peak of the EPSC. Measurements were performed on 5 to 10 consecutive EPSCs in the absence and presence of ifenprodil. Statistics were done using unpaired two-tailed *t*-tests or ANOVA. Significance was set at $P<0.05$. Data are reported as means ± standard errors (SE).

Materials and Methods, Chapter 2:

Breeding and cell culture

Because mice lacking both ε2 alleles die soon after birth, heterozygous ($\varepsilon2^{+/-}$) mice in a C57BL/6 background were used for generating $\varepsilon2^{-/-}$ mice. The heterozygous mouse colony was derived from $\varepsilon2^{+/-}$ mice that were a gift from Dr. Masayoshi Mishina (Kutsuwada et al., 1996). Hippocampal neurons from neonatal $\varepsilon2^{-/-}$ mice were rescued and grown in microisland cultures to examine the postsynaptic phenotype of $\varepsilon2^{-/-}$ neurons. Litters from heterozygous matings delivered 19-19.5 days after mating plugs were detected and ranged from 5-11 pups. Because mice lacking the ε2 subunit are unable to nurse (Kutsuwada et al., 1996) and $\varepsilon2^{+/-}$ mothers rarely nursed their pups, neurons from each newborn pup were cultured individually, with tissue preserved for genotyping (see below). All cultures were done using newborn animals. As previously described (Bekkers and Stevens, 1991) hippocampi from these animals were removed, enzymatically (papain; Collaborative Research) and mechanically dissociated and plated in microisland culture. The microisland substrate was prepared by spraying agarose-coated glass coverslips with poly-lysine and collagen. Neurons were plated at low density on this substrate to promote the formation of 'autaptic' synapses. EPSCs were apparent 6-7 days after plating.

Genotyping

All genotyping was done using polymerase chain reaction (PCR) amplification of genomic DNA prepared from mouse tissue. Tissue samples were incubated in proteinase K (0.5 mg/ml; GibcoBRL) at 55° C for at least 12 hours. Samples were centrifuged and the supernatant was added to an equal volume of isopropanol to precipitate genomic DNA. The samples were spun again to pellet the DNA. The pellet was washed in ice cold 70% ethanol and allowed to dry. Genomic DNA was resuspended in TE buffer (10 mM Tris, 1 mM EDTA, pH 8.0) then added to the PCR mixture of each of two reactions. All samples were subjected to two separate reactions (see figure 1 for details). PCR analysis was done using *Taq* polymerase and Promega (Madison, WI) reagents. Reaction products were run on 2% agarose gels and visualized using ethidium bromide. Gel purification and sequencing of the reaction products yielded the expected DNA

sequences (data not shown). Primer sequences were thus: Primer 1; 5'-ATgAAgCCCA gCgCAgAgTg-3'; Primer 2; 5'-ATggAAgTCAT CTTTCTCgTg-3'; Primer 3; 5'-ggCTACCTgC CCATTCgACC ACCAAgCgAA AC-3'; Primer 4; 5'-AggACTCATC CTTATCTgCC ATTATCATAg-3'. The cycling conditions (Perkin-Elmer GeneAmp 2400, Foster City, CA) were 30 cycles of 94°C (melting) for 30 seconds, 67°C (annealing) for 40 seconds and 72°C (extension) for 50 seconds. The reaction solution contained Mg^{++} (2 mM), dNTPs (0.2 mM each), oligonucleotide primers (0.01 mg/ml each), *Taq* polymerase (2.5 units), reaction buffer (5 µL) and 2 µL of solubilized genomic DNA (50 µl final volume) in HPLC water. Each animal was genotyped using two reactions, as shown in Figure 1B.

Electrophysiology

The extracellular recording solution contained (in mM): NaCl, 168; KCl, 2.4; HEPES, 10; D-glucose, 10; $CaCl_2$, 0.2-2.6; glycine, 0.01-0.02; bicuculline methiodide (BMI), 0.01 and 6-nitro-7-sulphamoylbenzo[f]quinoxaline-2, 3-dione (NBQX), 0.005 (325 mmol/kg final osmolality; pH 7.4) in HPLC-grade water. The intracellular recording solution contained (in mM): K-gluconate, 150; $CaCl_2$, 1.418; $MgCl_2$, 2; EGTA, 10; HEPES, 10; Na_2ATP, 2 and GTP, 0.2 (320 mmol/kg final osmolality; pH 7.4). Recording electrodes (TW150F-6; World Precision Instruments, Sarasota FL) had resistances of 1-5 MΩ. Autaptic EPSCs were evoked using a depolarization (to +10 mV for 0.5 msec). Fast solution exchanges were made with quartz flow pipes mounted to a piezo-electric bimorph driven by a stimulus isolation unit (Winston Electronics, Palo Alto, CA). Flow pipes were placed 50-100 µm from the cell body. Recordings were done using an Axopatch 2C amplifier and pCLAMP acquisition software (Axon Instruments, Foster City, CA). Data were low-pass filtered at 2.5 kHz, collected at 5 kHz and analyzed using Axograph (Axon Instruments). Data from dose-response experiments were fitted with $I=I_{max}/[1+(EC_{50}/A)^n]$, where I is the current response, I_{max} is the maximum response, A is the glycine concentration and n is the Hill coefficient. Each concentration tested represents data from at least four neurons. For glycine and antagonist experiments, neurons were pre-equilibrated with the drug at the concentration being tested. Control (NMDA, 1 mM) and experimental responses (NMDA plus drug) were interleaved to control for possible run-down of the whole-cell current. Whole-cell current

amplitudes were measured by averaging three points on either side of the absolute peak current. All data are reported as mean ± SE and were compared using an unpaired Student's *t*-test. All data are from neurons ≤10 days *in vitro* (DIV). Because the occurrence of wild-type and $\varepsilon 2^{-/-}$ animals in the same litter was rare, data from wild-type neurons was obtained primarily from congenic animals rather than littermates of $\varepsilon 2^{-/-}$ animals. All salts and drugs were from Sigma (St. Louis, MO) except for BMI, NBQX, NMDA and ifenprodil (RBI, Natick, MA). Statistical comparisons were made using Student's *t*-test, with significance set at $p<0.05$.

Materials and Methods, Chapter 3:

Breeding

All mice were in a C57B/6 background. Breeding pairs of ε1-targeted mice were placed together in the same cage and females were subsequently checked for the presence of mating plugs. Mice of the e1 -/- e1+/- mice genotype did not breed well and so breeding pairs were continually housed together with periodic rotation of males amongst different cages. Quite frequently, females that had shown the presence of mating plugs often would not deliver within the expected gestation time. In these cases, signs of pregnancy were not always apparent. Breeding pairs of ε1-/- ε2+/- mice were used to generate mice lacking the ε1-/- and ε2-/- subunits. Mice from these pairings were genotyped by using the method for genotyping at the ε1 allele and at the ε2 allele (Tovar et al., 2000).

Genotyping and cell culture.

Genotyping and cell culture were done as in Chapter 2 methods. Genomic DNA was isolated as indicated (see Chapter 2). Primers used in the genotyping were thus: E1P1: 5'-TCT ggg gCC Tgg TCT TCA ACA ATT CTg TgC-3'; E1P3: 5'-CCC gTT AgC CCg TTg AgT CAC CCC T-3'; E1P4: 5'-ATT CTT TgA TAA ATA TgC AAT GTA Tgg ggg-3'; NeoP1: 5'-gCC TgC TTg CCg AAT ATC ATg gTg gAA AA-3'.

Electrophysiology

Whole cell patch clamp recording was performed as in chapter 2. For current-voltage relationship experiments, liquid-liquid junction potentials were corrected.

Materials and Methods, Chapter 4:

Neuronal cell culture

Microisland cultures were prepared as previously described (Bekkers and Stevens, 1991). Glass coverslips (28 millimeter) in 35mm culture dishes (Nunc) were coated with 0.15% agarose. Once the coverslips were dry, we used an atomizer to spray a solution of poly-D-lysine (0.1875 mg/ml in 17 mM acetic acid; Sigma) and collagen (0.05 mg/ml; Collagen Corporation, Redwood City, CA). The hippocampi from P0-P1 mice (C57B/6) were removed, enzymatically (papain; Collaborative Research) and mechanically dissociated, and plated on previously cultured glial feeder layers. Media was exchanged weekly.

Whole-cell recording and solutions

Whole-cell voltage clamp recordings were performed on mouse hippocampal neurons in culture for at least 6 days. All recordings were done at room temperature. Neurons were perfused with extracellular solution containing (in mM): 168 NaCl; 2.4 KCl; 10 HEPES; 10 D-glucose; 1.3-2.6 $CaCl_2$; 0.02 glycine and 0.01 bicuculline methiodide with no added magnesium (pH 7.4; 325 mmol/kg). AMPA receptor antagonists were not regularly used unless specified. Recording electrodes were pulled from borosilicate glass (TW150F-6; World Precision Instruments) and had resistances between 1 and 2.5 MΩ. Electrodes were filled with solutions containing (in mM): 150 K-gluconate; 1.4 $CaCl_2$; 2 $MgCl_2$; 10 EGTA; 10 HEPES; 2 Na_2 ATP and 0.2 GTP (pH 7.4 and osmolarity 320 mmol/kg). In some experiments, K-glutamate was substituted for K-gluconate. Latrunculin B (Calbiochem) was solubilized in DMSO and solutions were prepared fresh as needed. The final DMSO concentration for these solutions was 0.1%. Solutions were delivered by gravity-fed quartz flowpipes placed 50-100 μm from a neuron. Flowpipes were controlled by solenoid valves (General Valve Company) and an external timer (Winston Instruments). Flowpipe translations were made by an attached piezo-electric bimorph and driven by a stimulus isolation unit (Winston Instruments). Exchanges could be effected in 30-50 msec (data not shown). Ifenprodil and ketamine were from RBI. NMDA and all other antagonists, unless otherwise stated, were from Tocris Neuramin.

Whole-cell recordings were made using an Axopatch-1C amplifier and pCLAMP acquisition software (Axon Instruments). Data were low-pass filtered (eight-pole Bessel; Frequency Devices) at 2.5 kHz and acquired at 5-10 kHz. Autaptic EPSCs were evoked with a depolarizing step (+10 mV, 0.5 -1 msec). Unless otherwise stated, all experiments used a paired-pulse protocol. Pairs were given at a frequency of 0.125 Hz with an interstimulus interval of 100 msec. Measurements of NMDA-receptor mediated EPSCs were made using a 60 millisecond window placed well after the AMPA receptor-mediated EPSC (see Fig 1B). EPSC recovery was measured by comparing the mean of five EPSCs immediately after removal of MK-801 with five EPSCs after 50 subsequent stimuli. Data are expressed as percent of current before MK-801 application. Measurement of whole-cell currents was done using a 50 msec window placed 60-70 msec after the start of the agonist application. To control for inadequate voltage clamp in low affinity antagonist experiments, EPSC amplitudes of each neuron were also tested in subsaturating concentrations of high-affinity competitive antagonists (either D-AP5 or D-CPP; Tong and Jahr, 1994). For experiments where NMDA and MK-801 were co-applied, the saturating NMDA concentration (1mM) should result in activation of all receptors in the membrane. After four co-applications of NMDA and MK-801 (20 μM), the current amplitude is expected to be no more than 2% of control, based on the reduction of the mean open time in MK-801 (Rosenmund et al., 1993). Because this is the prediction for non-equilibrium situations, it is likely to be an underestimation of the extent of block in the case of relatively long (1 sec) agonist application. Because the EPSC deactivation is accelerated in an open-channel blocker like MK-801, the majority of the difference in measured amplitude between control EPSCs and the first EPSC in MK-801 is accounted for by the difference in charge transfer. When the EPSC in MK-801 (10 μM) was normalized, the charge in MK-801 was 39.5 ± 5.4% of control (n=4) indicating that at least 60% of the reduction from control is accounted for by this difference in charge transfer. Block by ketamine in our experiments was use-dependent. When ketamine (50 μM) and DL-AP5 (200 μM) were co-applied during EPSC stimulation, the ratio of the current after ketamine/AP5 (10 stimuli) to the current before was 1.2 ± 0.02, n=3. Thus, ketamine action in this case was independent of other blocking mechanisms (Orser et al., 1997). Unbinding of ketamine during the agonist application at -70 mV (as in Fig 3C, D and 4B) contributed little to the estimate of

ketamine-blocked channels. Following complete block by ketamine, the recovery of the whole-cell current at -70 mV during an agonist application (measured as per Fig. 3C, D) was ≤5% of control amplitude (data not shown). All recordings were done on neurons between 6-9 days in culture. Data are reported as mean ± SE and were compared using paired *t*-tests, with significance set at $P<0.05$.

Chapter 1

Abstract

Activity-dependent synaptic rearrangements during CNS development require NMDA receptor activation. The control of NMDA receptor function by developmentally-regulated subunit expression has been proposed as one mechanism for this receptor dependence. We examined the phenotype of synaptic and extrasynaptic NMDA receptors during the development of synaptic load using the NR2B-selective antagonist ifenprodil. In cultured rat hippocampal neurons when relatively few synapses had formed, the ifenprodil block of EPSCs was less than whole-cell currents, the latter of which included both synaptic and extrasynaptic receptors. At the same developmental stage, we found that extrasynaptic receptors outnumbered synaptic receptors by 3:1, thus whole-cell currents were dominated by the extrasynaptic population. We used the macroscopic kinetics of ifenprodil block to distinguish between the receptor populations. The ifenprodil kinetics of whole-cell currents from neurons before and during the development of synaptic load was comparable to whole-cell currents in HEK293 cells transfected with NR1 and NR2B cDNA, indicating that extrasynaptic receptors are largely NR1/NR2B heteromers. In contrast, synaptic receptors included both a highly-ifenprodil sensitive (NR1/NR2B) component as well as a second population with lower ifenprodil sensitivity; the reduced ifenprodil block of EPSCs was attributable to synaptic receptors with lower ifenprodil sensitivity rather than to the appearance of ifenprodil-insensitive (NR1/NR2A) receptors. Our data indicates that the synaptic NMDA receptor complement changes quickly after synapse formation. We suggest that synapses containing predominately NR1/NR2B heteromers represent 'immature' sites whereas mature sites express NMDA receptors with a distinct, presumably triheteromeric, subunit composition.

Introduction

The N-methyl-D-aspartate (NMDA) receptor is implicated in developmentally-associated synaptic rearrangements in the vertebrate central nervous system (CNS). Native NMDA receptors are assembled from NMDA-R1 (NR1) and NMDA-R2 (NR2) subunits (ζ and ε, in mouse; Kutsuwada et al., 1992). The expression pattern of these subunits changes during development (Monyer et al, 1994; Sheng et al, 1994), suggesting that NMDA receptors composed of particular subunit combinations may govern the time course of the critical period during cortical development (Sheetz and Constantine-Paton, 1994). In the hippocampus, mRNA for NR1 and NR2B is predominant at times when synapses are forming while mRNA for NR2A is low, then increases to plateau levels later in development (Monyer et al., 1994; McDonald and Johnston, 1990). NMDA receptor-mediated synaptic responses are not present in hippocampal slices from neonatal $NR2B^{-/-}$ mice (Kutsuwada et al., 1996) implying that NR2B is required for channel formation or synaptic localization of functional NMDA receptors. Consistent with this expression pattern, mice lacking NR1 or NR2B die soon after birth (Forrest et al., 1994; Kutsuwada et al., 1996).

The expression pattern of NMDA receptor subunits could influence the development, maintenance and stabilization of synapses by several potential mechanisms. In heterologous expression systems (Monyer et al, 1994; Krupp et al., 1998) NMDA receptor properties are dependent on subunit composition (for review, see McBain and Mayer, 1994). Likewise, changes in subunit composition may account for the acceleration of the decay of NMDA receptor-mediated excitatory postsynaptic currents (EPSCs) seen during development (Carmingnoto and Vicini, 1992; Hestrin 1992). Receptor regulation by intracellular signaling cascades may also be subunit-specific. For example, the non-receptor tyrosine kinases *src* or *fyn* differentially regulate receptors containing NR2A or NR2B subunits (Kohr and Seeburg, 1996). Alternatively, NMDA receptors may play a structural role by specific interactions of their intracellular carboxy-terminal domains with postsynaptic density (PSD) proteins and sub-synaptic signaling machinery (Wyszynski et al., 1997; Sheng and Wyszynski, 1997; Ziff, 1997). Such a structural role might explain the observation that mice lacking the long intracellular carboxy-terminal domain of

NR2A or NR2B show the same phenotype as the respective targeted deletions (Sprengel et al, 1998).

Studies of recombinant NMDA receptors have provided pharmacological reagents that can distinguish between receptors containing different NR2 subunits. One of the most extensively studied of these is the noncompetitive antagonist ifenprodil. *Xenopus* oocytes expressing NR1/NR2B diheteromers are 400-fold more sensitive to ifenprodil than NR1/NR2A diheteromers (Williams, 1993). We took advantage of this selectivity and the kinetics of ifenprodil block to examine the role of NR2B-containing receptors during the period of synapse formation. NMDA receptor EPSCs and whole-cell currents were recorded in rat hippocampal neurons that formed autapses in single neuron microcultures. Our results indicated that highly ifenprodil-sensitive NR1/NR2B diheteromers comprise the initial extrasynaptic population whereas a second population of less ifenprodil-sensitive receptors are incorporated quickly after synapse formation.

Results

NMDA receptor-mediated EPSCs are less sensitive to ifenprodil than whole-cell NMDA currents.

We used whole-cell voltage clamp recording to compare the sensitivity of synaptic and whole-cell NMDA currents to the subunit-specific antagonist ifenprodil. Using microisland cultures, functional synaptic contacts were detected 4-5 days after plating, as judged by the presence of spontaneous and evoked EPSCs. Neurons continued to form synapses for 2-3 weeks *in vitro*, as judged by the increase in EPSC amplitude and by the increase in the number of GluR1-like immunoreactive puncta (data not shown). At 5-7 DIV, ifenprodil (3 μM) reversibly reduced the slow NMDA receptor-mediated component of the EPSC (Fig. 1A). This concentration of ifenprodil provides a maximal and selective block of NR1/NR2B diheteromeric receptors in heterologous expression systems (Williams, 1993; see below). However, the inhibition of EPSCs was quite variable, ranging from 15-50% of control, as shown for two different neurons in figure 1A. The average inhibition (I_{ifen}) was 30.2 ± 2.2% of control (n=22). Ifenprodil had no effect on the fast AMPA receptor-mediated component (94.1 ± 2.3% of control, n=3, Fig. 1B). Additionally,

ifenprodil did not alter the paired-pulse ratio (P_2/P_1: 1.38 ± 0.16 for control and 1.25 ± 0.13 for ifenprodil, n=4; 50 msec interstimulus interval) indicating that ifenprodil reduced NMDA receptor-mediated EPSCs by direct block of NMDA receptors rather than by a reduction of transmitter release.

For comparison, we measured the extent of ifenprodil block (3 μM) in a pure population of NR1/NR2B receptors by transfecting HEK293 cells with NR1 and NR2B cDNA. As expected, ifenprodil reduced steady-state NMDA-evoked (1 mM, 20 sec) currents to 17.5 ± 2.2% of control (n=14; Fig. 1C, D). Prior to synapse formation (1-3 DIV) and after synapse formation has begun (5-7 DIV), I_{ifen} from whole-cell currents in neurons was not significantly different than I_{ifen} in recombinant receptors (11.6 ± 0.9%, n=10 and 21.2 ± 2.1%; n=17, respectively; Fig 1C, D). Non-equilibrium agonist applications (1 mM glutamate, 100 msec) in the continuous presence of 3 μM ifenprodil resulted in a similar extent of block; I_{ifen} was 15.1 ± 1.0% (n=9) of control (data not shown). The extent of block of whole-cell currents in hippocampal neurons at 1-7 DIV is consistent with these currents resulting primarily from NR1/NR2B receptors. In neurons from 5-7 DIV, EPSCs were significantly less sensitive to block by ifenprodil than whole-cell currents. The difference in the ifenprodil sensitivity between synaptic and whole-cell NMDA receptors implies that the synaptic receptor complement includes NMDA receptors that are less sensitive or insensitive to ifenprodil.

Synaptic and extrasynaptic NMDA receptors are differentially-sensitive to ifenprodil.

Once synapses have formed, whole-cell currents reflect openings of synaptic as well as extrasynaptic NMDA receptors. Differences in subunit composition between these two receptor populations could explain the discrepancy in ifenprodil sensitivity if whole-cell currents predominantly reflect the gating of extrasynaptic receptors. We took advantage of the single axon input of microisland cultures to directly compare the ifenprodil sensitivity of the EPSC (synaptic) and whole-cell (synaptic plus extrasynaptic) current on the same neuron. As shown in figure 2A, there was not an obvious correlation between ifenprodil block of EPSCs and whole-cell currents on a given neuron but the peak whole-cell current was 55.6 ± 17.7 times larger than the EPSC in the same cell (Fig 2B, n=7). If all the receptors were synaptic, the EPSC would be expected to be 5-

fold smaller than the whole-cell current, assuming that the weighted average probability of transmitter release (P_r) at these terminals is approximately 0.2 (Rosenmund et al., 1993). However, the corrected amplitude of EPSCs is still an order of magnitude less than the whole-cell current, indicating that most of the functional NMDA receptors are extrasynaptic at this early stage of development.

To determine the ratio of extrasynaptic to synaptic receptors, we measured the peak current in response to 1 mM NMDA before and after irreversibly blocking the EPSC (in excess of 90%) with the use-dependent antagonist MK-801 (Huettner and Bean, 1988). Using this protocol (Fig 2C), the contribution of synaptic receptors was eliminated from the whole-cell response. In 4 cells, the whole-cell current remaining after block of the EPSC was 74.5 ± 2.1% of control, indicating that extrasynaptic receptors outnumbered synaptic receptors by 3:1 when synaptic load is relatively low. These data indicate that the small fraction of synaptic receptors at this developmental stage have little impact on the ifenprodil sensitivity of the whole-cell current.

Macroscopic kinetics of ifenprodil block

The similar degree of block of neuronal whole-cell currents and currents from NR1/NR2B recombinant receptors suggests that extrasynaptic receptors are NR1/NR2B diheteromers. However, the pharmacological similarity does not exclude other possibilities such as multiple NMDA receptor types within the extrasynaptic population. A comparison of the macroscopic kinetic characteristics of ifenprodil block provides a more sensitive test of this hypothesis. Figure 3A shows the onset of ifenprodil block during a steady-state application of NMDA. The onset of block accelerated with the ifenprodil concentration and reached a similar maximum block in both native receptors and in NR1/NR2B diheteromers. In neurons, the onset of block in 1, 3 or 10 μM ifenprodil was fitted with a single exponential with time constants (sec) of 1.55 ± 0.09 (n=7); 1.41 ± 0.19 (n=18) and 0.32 ± 0.03 (n=7), respectively. The time constants (sec) for NR1/NR2B receptors were 2.12 ± 0.58 (n=5); 0.95 ± 0.08 (n=8) and 0.51 ± 0.27 (n=5), respectively (figure 3A). The onset of block was slightly slower in NR1/NR2B diheteromers at 1 μM ifenprodil, but not statistically different than neurons at higher concentrations. In some cases, a high concentration of ifenprodil (10 μM) resulted in a fast relaxation in native and recombinant

receptors possibly reflecting a different mode of block as previously observed at higher ifenprodil concentrations (Legendre and Westbrook, 1991).

To examine recovery from ifenprodil block, NMDA receptors were activated with 1 mM NMDA, then blocked with 3 μM ifenprodil in the continuous presence of NMDA (Fig 3B). After washout of ifenprodil, test pulses of NMDA (1 second duration) were applied every 10 seconds to monitor recovery. The time required for recovery to 50% of the control amplitude was 47.2 ± 5.8 sec (n=6) for neurons at ≤7 DIV and 52.4 ± 4.2 sec for NR1/NR2B diheteromers (n=5, Fig. 3C). Thus the macroscopic kinetics of ifenprodil binding and unbinding are comparable in receptors from 5-7 DIV neurons and recombinant NR1/NR2B receptors suggesting that extrasynaptic receptor complement is composed largely, if not exclusively, of NR1/2B diheteromers.

Differential ifenprodil sensitivity at 'mature' synapses.

The expression of the NR2A subunit is low in rat brain prior to the 7th postnatal day and then increases to plateau levels 12-21 days after birth (Monyer et al, 1994; Sheng et al., 1994). A similar pattern also occurs *in vitro* (Zhong et al, 1994; Li et al., 1998). Because recombinant NR1/NR2A receptors are insensitive to 3 μM ifenprodil (Williams, 1993), we examined whether the ifenprodil sensitivity of NMDA receptor-mediated EPSCs decreased during this period. NMDA receptor-mediated EPSCs at ≥13 DIV were significantly less sensitive to ifenprodil (I_{ifen} = 43.1 ± 3.6% of control, n=14) compared to EPSCs at ≤7 DIV (compare insets in Fig 4A, B). AMPA receptor-mediated EPSCs at mature synapses were unaffected by 3 μM ifenprodil (95.6 ± 4.5% of control currents, n=4) nor was the paired-pulse ratio (data not shown). We blocked synaptic receptors from ≥13 DIV neurons with MK-801 (10 μM) and found that the ifenprodil sensitivity of extrasynaptic receptors (I_{ifen} = 20.6 ± 4.9%, n=4; data not shown) was not different from the whole-cell ifenprodil sensitivity in ≤7 DIV neurons. Thus the differential NMDA receptor distribution is even more pronounced at ≥13 DIV than at ≤7 DIV.

The deactivation of NMDA receptor mediated EPSCs was faster at mature synapses as described in other preparations (Carmingnoto and Vicini, 1992; Hestrin, 1992). This acceleration was attributable to a larger fast component of deactivation rather than a change in time constants

(≤7DIV: τ_1=252.2 ± 21.4 msec; τ_2=43.7 ± 4.5 msec; τ_1/τ_2 amplitude=1.1 ± 0.14; ≥13 DIV: τ_1=303.3 ± 31.4 msec; τ_2=52.4 ± 2.1 msec; τ_1/τ_2 amplitude=1.7 ± 0.26).

The age-dependent reduction in ifenprodil sensitivity of EPSCs could result from a homogenous NMDA receptor population characterized by decreased ifenprodil sensitivity or to the presence of a pharmacologically distinct class of synaptic NMDA receptors such as ifenprodil-insensitive NR1/NR2A receptors. We used the recovery from ifenprodil block to distinguish between these possibilities. Recovery for whole-cell currents was slow and monophasic (Fig 3B) thus recovery of the ifenprodil-sensitive component of the EPSCs would be expected to be similarly slow. Likewise if receptors with distinct ifenprodil sensitivities contribute to the EPSC, the recovery time course might be expected to be multiphasic.

As expected, for EPSCs at ≤7 DIV where ifenprodil produced a large degree of block (22% of control, Fig. 4A) recovery from ifenprodil block was monophasic, with a time constant (τ_{slow}) of 88.6 ± 21.1 sec (n=11; Fig 4D). In contrast, for EPSCs showing a lower ifenprodil sensitivity at ≥13 DIV (59% of control, Fig. 4B), a rapid initial component of recovery was apparent, followed by a slow component (see figure 4C for normalized comparison of recovery). The slow component was fitted with a single exponential with a time constant of 78.8 ± 16.1 seconds (n=8), similar to τ_{slow} at ≤7 DIV (Fig 4D). We could not determine the time constant of the fast component because higher stimulation rates caused changes in the amplitude of the EPSC, consistent with altered transmitter release and/or receptor desensitization. However, the fast component was fully developed at 0.3 Hz (data not shown), suggesting a time constant of 1 second or less. The biphasic recovery was not limited to neurons at ≥13 DIV. A rapid component of recovery was observed for EPSCs at ≤7 DIV that had a lower ifenprodil sensitivity, in the range for EPSCs ≥13 DIV.

The slow component of recovery at both ≤7 DIV and ≥13 DIV is consistent with the presence of NR1/NR2B receptors at these synapses whereas the reduced ifenprodil sensitivity and fast component of recovery indicates that receptors with a different subunit composition, possibly NR1/NR2A/NR2B triheteromers, are also present. Consistent with this hypothesis, the fast component was larger for EPSCs that were less sensitive to ifenprodil. For EPSCs where the block by ifenprodil suggested a homogeneous population of NR1/NR2B receptors (I_{ifen}<25% of

control), the fast component contributed 12.6 ± 1.9% (n=7). For EPSCs that were less ifenprodil-sensitive (I_{ifen}>25% of control), the fast component was 33.3 ± 3.7% (n=16; Fig. 4E).

Ifenprodil sensitivity of triheteromeric receptors containing NR1, NR2A and NR2B

A comparison of the ifenprodil sensitivity of native receptors with recombinant NR1/NR2 diheteromers is straightforward if native receptors consist of either highly-sensitive NR1/NR2B receptors or ifenprodil-insensitive NR1/NR2A receptors. However, native receptors can contain both NR2A and NR2B subunits (Sheng et al, 1994). Whether triheteromeric receptors composed of NR1, NR2A and NR2B are as sensitive to ifenprodil as NR1/NR2B receptors is unknown. To address this question, we transfected HEK293 cells with 1:1, 1:10 and 1:100 ratios of cDNA for NR2A:NR2B, along with NR1, and compared the ifenprodil sensitivity with cells transfected with NR1/NR2A and NR1/NR2B. As expected, recombinant NR1/NR2A receptors in our experiments were not blocked by ifenprodil (100.7 ± 5.7% of control, n=10, Fig. 5A,B) whereas NR1/NR2B receptors were highly sensitive (Fig. 2C, 5B). Cells transfected with both NR2A and NR2B showed intermediate sensitivities. I_{ifen} was 75 ± 4.1% of control (n=33) for a 1:1 ratio of NR2A:NR2B and 76.4 ± 4.2% of control (n=19) for a 1:10 ratio. The inhibition by ifenprodil for the 1:100 ratio was greater (35 ± 2.7% of control, n=15, Fig. 5B). However, the responses from these cells appeared to fall into two groups (figure 5C, D). In 8 cells, I_{ifen} was 10 ± 3.1% of control, similar to results from NR1/NR2B diheteromers whereas the remaining 7 cells had an intermediate ifenprodil sensitivity (48.4 ± 5.4% of control). The receptor complement in the highly ifenprodil-sensitive cells most likely represented NR1/NR2B diheteromers. As there was 100 times more NR2B cDNA, these cells probably did not receive sufficient NR2A-containing plasmid to affect the whole-cell current. However, the cells with intermediate ifenprodil sensitivity suggest an additional population of triheteromeric receptors.

For ratios of 1:1 and 1:10, the intermediate ifenprodil sensitivity could result from a mixed population of ifenprodil-insensitive NR1/NR2A and ifenprodil-sensitive NR1/NR2B receptors. In this case, the recovery from block should match NR1/NR2B receptors. We tested this possibility by examining the recovery from block from cells transfected with a 1:1 ratio of NR2A:NR2B (Fig. 6A). The half-recovery times for cells transfected with a 1:1 ratio of

NR2A/NR2B was much faster (0.49 ± 0.28 sec, n=7) than NR1/NR2B diheteromers (Fig. 6B). Thus these experiments indicate the presence of triheteromeric NR1/NR2A/NR2B receptors with an intermediate ifenprodil sensitivity.

Discussion

The microdot culture system allowed us to compare EPSCs and whole-cell currents from neurons during the development of synaptic load. Our data are consistent with the NMDA receptor complement being composed largely of NR1/NR2B diheteromers prior to synapse formation. Soon after synapse formation begins, the majority of NMDA receptors are still extrasynaptic and highly ifenprodil-sensitive. However, the synaptic NMDA receptor complement differs in its ifenprodil sensitivity due to the rapid appearance of less ifenprodil-sensitive (possibly triheteromeric) receptors. The addition of less ifenprodil-sensitive receptors while synaptic load is increasing may indicate that NMDA receptors incorporating NR2A subunits are localized at synaptic sites soon after synapses become functional.

Comparison to prior data

Our results rely on the subunit-specificity of ifenprodil. Previous results in heterologous expression systems indicate that ifenprodil at the concentrations used in our experiments maximally blocks NR1/NR2B receptors without affecting NR1/NR2A receptors (Williams, 1993). This was confirmed in our experiments with recombinant receptors expressed in HEK293 cells. Whole-cell currents in cultured hippocampal neurons were blocked by ifenprodil as previously demonstrated (Legendre and Westbrook, 1991). Based on their similar degree of block and macroscopic kinetics, we conclude that extrasynaptic receptors at 5-7 DIV are largely composed on NR1/NR2B diheteromers, consistent with the early expression of the NR2B subunit (Monyer et al., 1994; Kew et al. 1998).

Ifenprodil has recently been used to study native NMDA receptor subunit composition as well as developmental changes in NMDA receptor phenotype. In whole-cell recordings of acutely isolated cortical neurons, a developmental shift in ifenprodil sensitivity and a reduction

in glycine affinity was coincident with an increase in NR2A expression (Kew et al., 1998). The authors also reported that ifenprodil had a biphasic dose-response curve in neurons from older animals. Decreased glycine affinity is consistent with increased expression of NR2A (Kutsuwada et al., 1992). A two-component mechanism was also responsible for ifenprodil block of EPSCs in CA1 pyramidal neurons in slices from 7-28 day old mice (Kirson and Yaari, 1996). The ratio of high to low ifenprodil-sensitive components decreased in neurons from animals older than 35 days. Plant et al. (1997) found that EPSCs in GABAergic forebrain neurons in slice recordings from 14-17 day old rats were highly variable in their sensitivity to ifenprodil (3 μM, range 48-93% block). These results are consistent with our results indicating that synapse formation triggers heterogeneity in the synaptic NMDA receptor population.

Using whole-cell currents to inform us about synaptic NMDA receptors initially seemed like a reasonable strategy as synaptic NMDA receptors outnumber extrasynaptic receptors by 4:1 on neurons at 9-14 DIV (Rosenmund et al., 1995). However, direct measurement of the extrasynaptic/synaptic ratio at 5-7 DIV indicated that the majority of receptors were extrasynaptic. Whole-cell currents at this stage predominantly reflect the properties of extrasynaptic receptors thus do not provide an accurate sampling of synaptic receptors. The lower ifenprodil sensitivity of synaptic receptors compared to extrasynaptic receptors implies that there is rapid incorporation of pharmacologically distinct NMDA receptors into synaptic sites. Using a different approach, Stocca and Vicini (1998) have come to similar conclusions regarding NMDA receptor-mediated EPSCs in cortical slices. Whether the incorporation of new, presumably triheteromeric receptors occurs at synapses already containing NR1/NR2B receptors remains to be determined.

Role of NR2B and implications for synapse formation and maturation

Mice lacking NR2B die soon after birth and have no detectable NMDA receptor component of the excitatory postsynaptic potential (EPSP; Kutsuwada et al., 1996). This probably results from an inability to form functional channels rather than a general defect in localization of synaptic receptors because cultured neurons from these mice have NMDA receptor-mediated

EPSCs, with properties that are consistent with expression of NR1/NR2A diheteromers (Tovar et al., 1998).

Proteins that bind to intracellular domains of NMDA receptor subunits have recently been identified (see Gomperts, 1996; Ziff 1997 for reviews). Many of these proteins have homology to signal transduction molecules while others may anchor these transduction molecules to the PSD. Mice lacking the NR2A subunit have attenuated long-term potentiation (LTP) and are deficient in some learning paradigms but are otherwise viable (Sakimura et al., 1995). The deficiency in LTP in mice lacking NR2A could result from the lack of an anchoring or association site for molecules important in LTP. The NR2A and NR2B subunits both contain a PDZ-binding sequence required for attachment to that class of 'scaffolding' proteins (Kornau et al., 1995). However, in hippocampal neurons, the commonly expressed PDZ-containing protein, PSD-95, must not be initially responsible for clustering of NMDA receptors at synapses because immunocytochemical colocalization of PSD-95 with NMDA receptor subunits does not occur until 21 DIV (Rao et al., 1998). Our results indicate that synapses containing AMPA and NMDA receptor components have formed long before that time.

In contrast to our work, Rao and Craig (1998) used immunocytochemistry to demonstrate that NR2A- and NR2B-containing clusters become localized at sites opposite clusters of the presynaptic marker synaptophysin after 14 DIV. They inferred from this that synaptic localization of NMDA receptors does not occur until that time, and after localization of AMPA receptors (as inferred from clusters of the AMPA receptor subunit GluR1). However, our results indicate that functional synapses form after 5 days in culture, that NMDA receptors are present at these nascent synapses and that NR2B subunits initially predominate at these sites. The differences between the physiological and immunocytochemical results may arise from an inability to detect with immunohistochemical methods, small numbers of receptors at nascent synapses.

Nascent and Mature Synapses

We present the following hypothesis for formation and maturation of the synaptic NMDA receptor complement in our system: Nascent synaptic NMDA receptors are NR1/NR2B

diheteromers. This is likely because prior to synapse formation the properties of NMDA receptors are similar to those of recombinant NR1/NR2B receptors. Once a synapse has formed, activity at that synapse results in incorporation of another NMDA receptor type, NR1/NR2A/NR2B trihetetomers which are specifically targeted to synapses. A corollary of this hypothesis, not tested directly by our experiments, is that synapses initially form promiscuously. Only after they have formed does input-dependent alteration of the NMDA receptor phenotype at that synapse occur. Our model does not consider the possible role for the newly discovered NR3 subunit which is developmentally expressed (Das et al., 1998)

Our model implies that an input-dependent event occurs such that the synaptic receptor complement changes at functional synapses. This is directly analogous to the developing neuromuscular junction (NMJ) where acetylcholine receptor (AChR) channel kinetics (Cull-Candy et al., 1982; Brenner and Sakmann, 1983) differ between extrasynaptic and synaptic populations of channels. Changes in the kinetic properties of ACh channels are thought to result from factors provided by the presynaptic nerve terminal (Brenner and Sakmann, 1983). For a central excitatory synapse, the nature of the presynaptic signal may be activity at that synapse or a factor from the presynaptic terminal analogous to ARIA (acetylcholine receptor inducing activity; see Fischbach and Rosen 1997) at the NMJ. The maturation of EPSC kinetics and their pharmacological properties at cultured CA1 hippocampal neurons seems to be dependent on tetanus toxin-sensitive exocytosis (Lindlbauer et al., 1998; see also Gottman et al., 1997), consistent with this idea. Recently a member of the ARIA family, neuregulin-β, has been implicated in changes in NMDA receptor subunit expression that occur in cerebellar granule cells (Ozaki et al, 1997). In support of the idea that NMDA receptor activity results in changes in the receptor complement at active synapses, hippocampal neurons cultured in AP5 show a heightened sensitivity to ifenprodil, as if NMDA receptors at all synaptic sites were pure NR1/NR2B diheteromers (Chavis and Westbrook, 1998).

Our evidence indicates that nascent synapses are homogenous with respect to their NMDA receptor complement. A model of cortical development holds that changes in NMDA receptor subunit composition are important in governing the period during which synaptic rearrangements can occur (Sheetz and Constantine-Paton, 1994). An elaboration of this model is

that sites with more than one type of NMDA receptor are the very sites that are capable of being modified and they are marked by the presence of NR2A-containing receptors. This is supported by the apparent speed with which NR2A-containing receptors appear at synapses in this study (see also Stocca and Vicini, 1998). Blockade of NMDA receptors *in vivo* prevents the formation of topographic maps (Kleinschmidt et al., 1987; Cline et al., 1987) and also prevents the change from high to low NMDA EPSC ifenprodil sensitivity (Chavis and Westbrook, 1998). If NMDA channel gating acts upon the same mechanisms in these systems, neural activity at synapses containing di- and triheteromeric NMDA receptors may be required for the formation of correlation-based topographic maps. Thus NR1/NR2B-only synapses may mark new synapses available for further elaboration and synapses with di- and triheteromeric receptors may mark synapses that are subject to correlation-based refinement. The limit of correlation-based synaptic refinement (i.e. the critical period duration) may occur when synapses contain only triheteromeric receptors.

Chapter 2

Abstract

The NMDA receptor has been implicated in the formation of synaptic connections. To investigate the role of the ε2 (NR2B) NMDA receptor subunit, which is prominently expressed during early development, we used neurons from mice lacking this subunit. Although $\varepsilon2^{-/-}$ mice die soon after birth, we examined whether NMDA receptor targeting to the postsynaptic membrane was dependent on the ε2 subunit by rescuing hippocampal neurons from these mice and studying them in autaptic cultures. In voltage-clamp recordings, excitatory postsynaptic currents (EPSCs) from $\varepsilon2^{-/-}$ neurons expressed an NMDA receptor-mediated EPSC that was apparent as soon as synaptic activity developed. However, compared to wild-type neurons, NMDA receptor-mediated EPSC deactivation kinetics were much faster, were less sensitive to glycine, but were blocked by Mg^{++} or AP-5. Whole-cell currents from $\varepsilon2^{-/-}$ neurons were also more sensitive to block by low concentrations of Zn^{++} and much less sensitive to the ε2-specific antagonist ifenprodil than wild-type currents. The rapid NMDA receptor-mediated EPSC deactivation kinetics and the pharmacological profile from $\varepsilon2^{-/-}$ neurons are consistent with the expression of ζ1/ε1 diheteromeric receptors in excitatory hippocampal neurons from mice lacking the ε2 subunit. Thus ε1 can substitute for the ε2 subunit at synapses and ε2 is not required for targeting of NMDA receptors to the postsynaptic membrane.

Introduction.

N-methyl-D-aspartate (NMDA) receptors are composed of two subunit types, ζ and ε (or NR1 and NR2 in rat). In the rodent hippocampus, ε1 and ε2 are the predominantly expressed ε subunits in excitatory neurons (Monyer et al., 1994; but see Das et al., 1998). Mice lacking the ε2 subunit ($\varepsilon 2^{-/-}$) die soon after birth but can survive for a few days with hand-feeding. Hippocampal slices obtained from these mice at postnatal day 3 lack a synaptic NMDA receptor-mediated component (Kutsuwada et al., 1996), indicating that early in development, ε2-containing receptors are required either for formation of functional NMDA receptors or synaptic localization of receptors. Mice lacking the intracellular C-terminal domain of ε2 show a similar phenotype (Sprengel et al., 1998), providing further evidence for a role of the ε2 subunit in targeting to the postsynaptic density (PSD). In contrast, mice lacking the ε1 subunit are viable but have attenuated long-term potentiation (LTP; Sakimura et al., 1995). The ε1 subunit is detected at very low levels in early development (Monyer et al, 1994; Li et al, 1998), but NMDA receptors containing the ε1 subunit are incorporated into the synaptic receptor complement soon after synapses have begun to form *in vitro* (Stocca And Vicini, 1998; Tovar and Westbrook, 1999). We now report that neurons, cultured from $\varepsilon 2^{-/-}$ mice express NMDA receptor-mediated EPSCs with unusually rapid deactivation kinetics and distinctive pharmacological properties, consistent with expression of ζ1/ε1 diheteromeric receptors. Thus, the ε2 subunit is not required for the formation of dual-component EPSCs. Likewise, incorporation of NMDA receptors at synapses can occur independently of the ε2 subunit.

Results

Genotyping ε2-Targeted Mice

Figure 7A shows the organization of ε2 wild-type and targeted alleles and the alignment of the PCR primers. The primers were designed to amplify the designated genomic DNA regions

of wild-type and targeted alleles across insert/wild-type junctions. Two separate PCRs were used to determine the genotype of each animal. Each PCR was designed to amplify a different pair of reaction products (bracketed lanes in Fig 7B). This resulted in a unique pair of reactions for $\varepsilon2^{+/+}$ and $\varepsilon2^{-/-}$ animals, while $\varepsilon2^{+/-}$ animals had 4 reaction products. Genotypes from progeny of heterozygous mice pairings were 22 ($^{+/+}$):70 ($^{+/-}$):24 ($^{-/-}$), not significantly different from a Mendelian distribution (using χ^2 criteria). Genotyping of outbred litters (resulting from $\varepsilon2^{+/-}$ and wild-type pairings) produced a wild-type to heterozygote ratio of 43:31, indicating that our genotyping method did not favor the production of reaction products from the targeted allele.

NMDA Receptor-Mediated EPSCs from $\varepsilon2^{-/-}$ Neurons

EPSCs in wild-type hippocampal neurons have two kinetically distinct components. The fast component (deactivation τ: ca. 1-5 msec) results from the activation of AMPA receptors while the slow component (deactivation τ: ca. 40 and 300 msec) results from NMDA receptor activation (McBain and Mayer, 1994). In $\varepsilon2^{-/-}$ neurons, EPSCs were apparent in microisland cultures after 6-7 days. However, the decay of the EPSC did not show two distinct kinetic components, characteristic of AMPA and NMDA receptor-mediated EPSCs in wild-type neurons. The NMDA receptor antagonist AP5 markedly shortened the decay of the dual-component EPSC in wild-type neurons (Fig. 8A) but had a much less profound effect on the decay in $\varepsilon2^{-/-}$ neurons (Fig. 8B). The AP5-sensitive components from wild-type and $\varepsilon2^{-/-}$ neurons are superimposed in Figure 8C. The deactivation kinetics of NMDA receptor-mediated EPSCs from wild-type neurons (Fig. 8A, C) were well-fitted with two exponentials (τ_f = 42.4 ± 3.6 msec; τ_s = 288.8 ± 24.1 msec, n = 15), similar to cultured rat neurons (e.g. Tovar and Westbrook, 1999). In contrast, the deactivation kinetics of EPSCs from $\varepsilon2^{-/-}$ neurons (Fig. 8B) were dramatically faster (τ_f = 20.6 ± 1.7 msec; τ_s = 100.8 ± 13.6 msec, n = 7). For NMDA receptor-mediated EPSCs from $\varepsilon2^{-/-}$ neurons, the sum of squared errors (SSE) for two-exponential fits was 9.9 ± 3.4 times better than for a single exponential fit. In $\varepsilon2^{-/-}$ neurons, the deactivation kinetics were dominated by τ_f. The ratio (τ_f/τ_s) was 6.04 ± 1.09 (n = 7) for $\varepsilon2^{-/-}$ neurons and 1.16 ± 0.15 (n = 15) for wild-type neurons. Although the deactivation kinetics from $\varepsilon2^{-/-}$ neurons were usually well-fitted with two exponentials, in two cases the deactivation could be fitted with a single exponential (t≈34 msec). The fast deactivation kinetics of NMDA

receptor-mediated EPSCs in $\varepsilon2^{-/-}$ neurons are consistent with deactivation kinetics expected of recombinant $\zeta1/\varepsilon1$ diheteromeric receptors (Vicini et al., 1998) and are much faster than EPSC deactivations seen in other preparations (McBain and Mayer, 1994; see however, Bardoni et al., 1998). Consistent with an NMDA receptor-mediated EPSC, currents from $\varepsilon2^{-/-}$ neurons became larger by increasing extracellular glycine (n=4) and were completely blocked by Mg^{++} (n=4; Fig 8D).

Pharmacology of $\varepsilon2^{-/-}$ NMDA Receptors is Consistent with $\zeta1/\varepsilon1$ Receptors

Experiments using recombinant receptors have provided pharmacological tools that can be diagnostic for specific diheteromeric subunit combinations. We used glycine (Kutsuwada et al., 1992), Zn^{++} (Paoletti et al., 1997) and ifenprodil (Williams, 1993) to investigate the subunit composition of NMDA receptors from $\varepsilon2^{-/-}$ neurons.

Recombinant $\zeta1/\varepsilon1$ receptors are more than ten-fold less sensitive to glycine than $\zeta1/\varepsilon2$ receptors (Kutsuwada et al., 1992). We measured the deactivation of whole-cell glycine-evoked currents from $\varepsilon2^{-/-}$ and wild-type neurons (Fig 9A) using fast application methods. Glycine deactivations from $\varepsilon2^{-/-}$ neurons decayed quickly and were well-fitted by single exponentials (0.11 ± 0.1 sec, n=6) while the deactivations from wild-type neurons were slower and required two exponential components to be well-fitted (τ_f=0.266 ± 0.2 sec, τ_s=1.38 ± 0.06 sec, n=6). This is consistent with an 8 to 10-fold faster glycine microscopic unbinding rate in receptors from $\varepsilon2^{-/-}$ neurons. We confirmed the lower glycine affinity of receptors from $\varepsilon2^{-/-}$ neurons by comparing the glycine dose-response relationship for $\varepsilon2^{-/-}$ (EC_{50} = 3.61 μM) with wild-type (EC_{50} = 0.14 μM) neurons (Fig. 9A). The EC_{50} value for $\varepsilon2^{-/-}$ NMDA receptors is consistent with that of $\zeta1/\varepsilon1$-containing NMDA receptors (Kutsuwada et al., 1992).

Recombinant $\zeta1/\varepsilon1$ receptors are also selectively antagonized in a voltage-independent manner by nanomolar Zn^{++} (Paoletti et al., 1997). Because the IC_{50} for high-affinity Zn^{++} antagonism is near the levels of contaminating Zn^{++} (Paoletti et al., 1997), the high-affinity Zn^{++} chelator TPEN (1 μM) was included in the control solution. Whole-cell NMDA (1 mM) currents from wild-type neurons (Fig. 9B) were reduced slightly in Zn^{++} (500 nM; 80.8 ± 3.0% of control, n = 6) whereas currents from neurons lacking $\varepsilon2^{-/-}$ were almost completely blocked (18.1 ± 1.8% of

control, n=6). In contrast, the selective ζ1/ε2 receptor antagonist ifenprodil (3 μM: Williams, 1993) reduced whole-cell NMDA (1 mM) currents from wild-type (33.3 ± 6.0% of control, n=8) to a much greater extent than currents from $\varepsilon2^{-/-}$ neurons (85.2 ± 1.7%, n=5; Fig 9C). Thus, the pharmacological profile of $\varepsilon2^{-/-}$ NMDA receptors is consistent with that expected from ζ1/ε1 heteromers.

Discussion

NMDA receptor-mediated EPSCs from cultured hippocampal neurons lacking the ε2 subunit have very fast deactivation kinetics compared to those from wild-type neurons. Fast NMDA receptor-mediated EPSC kinetics have been reported in wild-type animals but seem to be the exception rather than the norm. EPSC deactivation kinetics similar to those reported here occur during synapse formation in the rat spinal cord (Bardoni et al., 1998) and cerebellar granule cells (D'Angelo et al., 1993). Additionally, EPSC deactivation kinetics recorded from mature synapses on cerebellar granule neurons from mice lacking the ε3 (NR2C) subunit are very similar to those that we report from $\varepsilon2^{-/-}$ neurons (Ebralidze et al., 1996). NMDA receptor-mediated EPSC deactivation kinetics in other preparations are comparable to our results from wild-type neurons. The slow kinetics of the NMDA receptor-mediated EPSC have been thought to account for rhythmic, pacemaker activities like breathing, locomotion and suckling, arising from central pattern generators in brainstem nuclei and the spinal cord. However, the neonatal death in mice lacking the ε2 subunit most likely results from the absence of synaptic NMDA receptors in regions otherwise expressing the ε2 subunit, rather than changes in deactivation kinetics.

Our data indicates that the ε2 subunit is not required for synaptic localization of NMDA receptors. Previous work with these animals reported a lack of the NMDA receptor-mediated component of the field EPSP in $\varepsilon2^{-/-}$ hippocampi from animals at postnatal day 2-3 (Kutsuwada et al., 1996). This is consistent with our observation that NMDA-evoked currents from $\varepsilon2^{-/-}$ neurons often do not appear until 4-5 DIV and ε1 is not expressed until after this time *in vivo* (Monyer et al., 1994; Sheng et al., 1994). The increase in expression of ε1 is coincident with the acceleration of

the wild-type NMDA receptor-mediated deactivation kinetics (Carmingnoto and Vicini, 1992; Hestrin 1992).

Based on the characteristics of NMDA receptor-mediated EPSCs, we propose that the NMDA receptors expressed in $\varepsilon 2^{-/-}$ neurons are $\zeta 1/\varepsilon 1$ diheteromeric receptors. If this is true, this means that the signals required for NMDA receptor targeting to the somato-dendritic membrane and/or synaptic localization of NMDA receptors are found on $\zeta 1$ or $\varepsilon 1$. The $\varepsilon 2$ subunit is required early in development because of a need for functional NMDA receptors rather than targeting (to the somato-dendritic membrane) or localization (to the postsynaptic membrane) of synaptic receptors. Targeting and localization events may require different amino acid sequence motifs. The carboxy-terminal intracellular regions of $\varepsilon 1$ and $\varepsilon 2$ have amino acid sequence homologies in the region just after the final transmembrane segment and at the PDZ recognition sites at the carboxy termini. Mice lacking the PDZ recognition sequences in $\varepsilon 2$ show decreased levels of synaptic NMDA receptors (Mori et al., 1998). This suggests that NMDA receptor targeting is retained but synaptic localization may be reduced. Furthermore, proteins that bind to the PDZ domain such as PSD-95 are not required for synaptic localization of these receptors. The AMPA receptor-mediated component appears normal in animals without the NMDA receptor-mediated component (Kutsuwada et al., 1996), indicating that incorporation of AMPA receptors at synapses is independent of NMDA receptor activation.

Chapter 3

Introduction

The expression pattern of NMDA receptor subunits is developmentally regulated as well being subject to influence by signaling factors (Ozaki, 1999) and by membrane depolarization (Bessho, 1994). In rodent excitatory hippocampal neurons the predominant subunits are ζ1, ε1 and ε2 ((NR1, NR2A and NR2B in rat). Expression of functional receptors requires expression of ζ1 and a member of the ε subunit family. Mice lacking the ζ1 or ε2 subunit die soon after birth (Forrest et al., 1994; Kutsuwada et al., 1996) whereas mice lacking the ε1 subunit, while having deficits in certain measures of synaptic plasticity (Sakimura et al., 1995) are viable. Neurons lacking the ζ1 subunit are unresponsive to NMDA (Forrest et al., 1994). Cultured hippocampal neurons lacking the ε2 subunit express receptors that have properties expected from receptors composed of ζ1 and ε1 subunits (Tovar et al., 2000). Moreover, excitatory postsynaptic currents (EPSCs) from neurons lacking ε2 have exceptionally fast deactivation kinetics not seen in wild type neurons which are presumably expressing ζ1, ε1 and ε2 (Tovar and Westbrook, 1999). Therefore, it appears likely that triheteromeric receptors containing all three receptor types form preferentially over diheteromeric receptors of either kind (ζ1/ε1 or ζ1/ε2) in wild-type neurons. In mammalian cells, the ζ1 subunit alone is thought to be incapable of forming functional channels. Thus by generating mice that lack the ε1 and ε2 receptors, it may be possible to create neurons that lack functional NMDA receptors.

Recent work indicates that early EPSCs can result from synapses that contain only NMDA receptors (Durand et al., 1996; Wu et al., 1996; Isaac et al., 1997). These sites have been termed 'silent synapse' because they lack AMPA receptors which are thought to relieve the magnesium block of the NMDA receptor. Conversion of silent synapses into functional ones by incorporation of AMPA receptors requires stimuli which also evokes long-term potentiation (Durand et al., 1996; Isaac et al., 1997). This work has led to the view that NMDA receptors are required for the formation of synapses, despite other evidence to the contrary (Segal and Furschpan, 1990; Li et al., 1994).

We examined these questions using cultured hippocampal neurons from mice lacking either the ε1 subunit or both the ε1 and ε2 subunits. By examining the properties of EPSCs from wild-type and $\varepsilon1^{-/-}$ neurons, we can infer the properties of triheteromeric receptors in wild-type neurons. We can verify that ζ1, ε1 and ε2 are the normal subunits expressed in these cells. Furthermore, if neurons lacking ε1 and ε2 also lack functional NMDA receptors we can ask whether NMDA receptors are required during the initial stages of synapse formation.

Results

Genotyping ε1-Targeted Mice

Genotyping of ε1-targeted mice was done in a manner similar to genotyping of ε2-targeted mice. We used the polymerase chain reaction (PCR) to amplify DNA products of predicted sizes. The organization of the ε1 wild-type and targeted alleles and the alignment of the PCR primers is shown in Fig 10A. As in genotyping of ε2-targeted mice, three primers were used in each reaction. With this scheme, products from wild-type and ε1 targeted genomic DNA could be amplified in every reaction, thereby insuring that a product was made in every reaction. Two independent reactions were performed per DNA sample from each mouse. Each PCR of these pairs contained unique primer combinations. The results from each separate reaction were run on agarose gels (2%), stained with ethidium bromide and visualized. As expected, crosses between mice lacking the ε1 subunit produced only $\varepsilon1^{-/-}$ mice while crosses between wild-type and $\varepsilon1^{-/-}$ mice produced mice in the expected Mendelian ratios (data not shown).

Mice

All mice were kept in a C57B/6 background. This was done by periodic out-breeding with wild-type animals from the C57B/6J background. Mice lacking the ε1 subunit appeared normal and were viable. However, males and females from these lines were prone to seizures. The seizures were often brought about when the animals were handled and would last 10-30 seconds. Most mice from this line exhibited this behavior but the behavior was not

lways seen in any particular animal. Seizures were never seen in wild-type mice.

We obtained animals lacking the ε1 and ε2 subunits with high frequency by crossing e1- and e2-targeted line to generate animals of the $\varepsilon1^{-/-}\varepsilon2^{+/-}$ genotype. We used these as mating pairs for creating the double knockout. When sexually mature, these mice could often be distinguished from wild-type mice by their behavior and appearance. Whereas wild-type mice scurry about their cage when their enclosures were moved, $\varepsilon1^{-/-}\varepsilon2^{+/-}$ mice would often remain motionless and would require gentle prodding to move about. This appeared to be a reluctance to move because $\varepsilon1^{-/-}\varepsilon2^{+/-}$ mice appearing to walk normally. Additionally, the coats of $\varepsilon1^{-/-}\varepsilon2^{+/-}$ animals appeared dull, oily and matted, compared to those of wild-type mice which were uniformly glossy. Interestingly, although the $\varepsilon1^{-/-}\varepsilon2^{+/-}$ mice were homozygous for the mutated ε1 allele, they never exhibited handling-evoked seizures as had $\varepsilon1^{-/-}$ mice.

To obtain neurons from $\varepsilon1^{-/-}\varepsilon2^{-/-}$ mice, we would discern which pups had nursed. This criteria was used because newborn $\varepsilon2^{-/-}$ pups are unable to nurse (Kutsuwada et al., 1996). The use of this criteria, however, often required that newborn pups be surrogated with wild-type females because $\varepsilon1^{-/-}\varepsilon2^{+/-}$ females would only infrequently nurse their pups. All the pups that lacked milk in their stomachs a few hours after birth were sacrificed for cell culture. Neurons from the hippocampi of each animal were cultured individually. At the time of the dissection, tails were removed from the pups and prepared for genomic DNA isolation. Other pups from these pairings were allowed to grow and their genotypes were determined following weaning. Because of these requirements for obtaining neurons from $\varepsilon1^{-/-}\varepsilon2^{-/-}$ mice, we never examine the lethality of the dual mutations. However upon genotyping of the littermates of these pups as juveniles, we never found any of mice that lacked ε1 and ε2. Thus it is likely that the dual mutation is lethal, as is the single ε2 mutation (Kutsuwada, 1996).

EPSCs From Neurons Lacking ε1.

We used the whole-cell voltage clamp configuration to record evoked autaptic EPSCs from $\varepsilon1^{-/-}$ neurons in microculture. These neurons grew normally and did not appear noticeably different from wild-type neurons at similar developmental stages. Synapses developed with the

same time course as in wild-type neurons and EPSCs from these neurons contained AMPA and NMDA receptor-mediated components.

NMDA receptor-mediated EPSCs from cultured hippocampal neurons lacking the ε1 subunit were consistent with the presence of receptors composed of the ζ1 and the ε2 subunits (Vicini et al., 1998). Deactivation kinetics of NMDA receptor-mediated EPSCs from $\varepsilon1^{-/-}$ neurons were uniformly slow compared to EPSCs from wild-type neurons (Figure 11A). The EPSC deactivation kinetics from neurons lacking ε1 were well-fitted with single exponentials in all cases (292.4 ± 13.3 msec, n=16). In contrast, EPSCs from most wild-type neurons (29/33) were fitted using two exponentials (τ_{slow}: 300.2 ± 12.94; τ_{fast}: 38.2 ± 4.032 msec, n=29). The remaining four neurons were not better fitted with two exponentials and showed a predominantly slow single exponential deactivation (223.6 ± 0.723 msec, n=4). The slow components of the fitted deactivation time constant from wild-type EPSCs and neurons lacking ε1 were not different (Fig 11B). In rat neurons, an acceleration in the deactivation kinetics occurs with time in culture and results from a greater fraction of the deactivation resulting from the fast component (Tovar and Westbrook, 1999). However, we did not see a comparable acceleration of the EPSCs in cultures from wild-type mouse neurons (τ_{fast}/τ_{slow}=1.33 ± 0.19 in neurons at 6-7 days in culture, n=13; τ_{fast}/τ_{slow}=1.20 ± 0.10 in neurons at 9-12 days in culture, n=17). This could reflect an acceleration in the developmental program of subunit expression in mice compared to rats.

The subunit specific antagonist ifenprodil (Williams, 1993) has been used to examine the subunit composition of native NMDA receptors containing the ε2 subunit (Kirson and Yaari, 1996; Plant et al., 1997) as well as being used to demonstrate a developmental switch in synaptic NMDA receptors (Tovar and Westbrook, 1999). In cultured mouse neurons, EPSCs were relatively ifenprodil insensitive (Fig 11C, top). However, EPSCs from neurons lacking the ε1 subunit were highly sensitive to ifenprodil even at a time (11 DIV) when the ifenprodil sensitivity would be expected to be diminished, based on work on rat neurons (Tovar and Westbrook, 1999). In these neurons, EPSC amplitudes were 22.7 ± 1.93% of control (n=4), consistent with the synaptic complement resulting from NR1/NR2B diheteromeric receptors. Interestingly, the ifenprodil sensitivity of wild-type mouse neurons at early times in culture (6-7 DIV) were much less sensitive to ifenprodil compared to rat neurons in similar conditions. Moreover, there was no

decrease in ifenprodil sensitivity with time in culture as observed in rat neurons. However this is not surprising considering the EPSC deactivation kinetics which correlate with ifenprodil sensitivity (Tovar and Westbrook, 1999). EPSCs from wild-type mouse neurons were much faster than would be expected if the ε2 subunit was incorporated into the synaptic receptor complement to any significant extent (Vicini et al., 1998). As predicted, however, EPSCs from $\varepsilon1^{-/-}$ neurons had properties consistent with the expression of ζ1/ε2 diheteromeric receptors at synapses.

EPSCs From Neurons Lacking ε1 and ε2.

We bred mice of the $\varepsilon1^{-/-}\varepsilon2^{+/-}$ genotype to obtain $\varepsilon1^{-/-}\varepsilon2^{-/-}$ mice with high frequency. Following cell culture and genotyping, identified neurons from $\varepsilon1^{-/-}\varepsilon2^{-/-}$ mice were used in electrophysiology experiments. In whole-cell recordings combined with flowpipe agonist application, the majority (22/23) of e1-/- e2-/- neurons showed no response to NMDA (1 mM, 1 sec; figure 12A). In the single case in which NMDA evoked a current, the response to NMDA was atypical in that it peaked much more slowly than normally seen in wild-type neurons, the deactivation was also much slower than normal and the current amplitude was much smaller that what would normally be expected from these neurons (data not shown). In all the $\varepsilon1^{-/-}\varepsilon2^{-/-}$ neurons tested, glutamate (100 μM) applications resulted in robust whole-cell currents.

AMPA receptor-mediated EPSCs were obvious in $\varepsilon1^{-/-}\varepsilon2^{-/-}$ neurons after 6-7 days in culture. In order to see an NMDA receptor contribution to the evoked EPSC, recordings we done in 20 μM glycine and no added magnesium or NMDA receptor antagonists. In no case did we observe NMDA receptor-mediated EPSCs (Fig 12B). The time course of the EPSC did not change with the addition of AP5 (200 μM) and there was no residual current upon the addition of an AMPA receptor antagonist (see Fig 12B). In all neurons tested, we were able to record either evoked AMPA receptor-mediated EPSCs or miniature excitatory postsynaptic currents (mEPSCs). Thus synapses form normally in the absence of the ε1 and ε2 subunits and, moreover, functional NMDA receptors.

We asked if synaptic AMPA receptors were noticeably altered by the absence of functional NMDA receptors. We did this by examining the properties of mEPSCs. As a control, we cultured wild-type neurons in AP5 (200 μM) to mimic the $\varepsilon1^{-/-}\varepsilon2^{-/-}$ situation. As shown (Fig

13A and B), mEPSCs displayed similar amplitudes (wild-type: 24.9 ± 1.7 pA, n=11; DKO: 36.4 ± 6.5, n=13; AP5-treated: 31.6 ± 4.0 pA, n=12) and deactivation kinetics (wild-type: 2.87 ± 0.07 msec, n=11; DKO: 2.78 ± 0.188 msec, n=13; AP5-treated: 3.15 ± 0.19, n=12) in all three conditions. Thus to a first approximation, synaptic AMPA receptor expression appeared unaffected by the lack of $\varepsilon1^{-/-}\varepsilon2^{-/-}$ or in wild-type neurons cultured in AP5.

We compared the current/voltage relationship in response to applications of AMPA (20 μM) of wild-type and $\varepsilon1^{-/-}\varepsilon2^{-/-}$ neurons. The absence of the GluR2 subunit of the AMPA receptor results in sensitivity of those receptors to voltage-dependent channel block by intracellular spermine (Washburn, 1997). Spermine sensitivity can be determined by the rectification characteristics from the current/voltage relationship. All neurons, responded to AMPA (20 μM). As seen (Fig 13C) the rectification characteristics of the wild-type (squares) and $\varepsilon1^{-/-}\varepsilon2^{-/-}$ neurons (circles) was different in both the absence (closed symbols) and the presence (open symbols) of spermine (1 mM). This likely represents a difference between wild-type and $\varepsilon1^{-/-}\varepsilon2^{-/-}$ neurons with respect to the GluR2 content within the AMPA receptor complement of the respective groups. This was the only difference that was apparent between wild-type and $\varepsilon1^{-/-}\varepsilon2^{-/-}$ neurons.

Chapter 4

Abstract

Glutamate receptors are concentrated in the postsynaptic complex of central synapses. This implies a highly organized postsynaptic membrane with tightly anchored neurotransmitter receptors. However, recent studies indicating that AMPA receptors can be rapidly cycled between intracellular pools and the plasma membrane during synaptic plasticity, have challenged this view (Lüscher et al., 1999; Shi et al., 1999). We report here that NMDA receptors at newly formed synapses also are not fixed, but rather move between synaptic and extrasynaptic domains. The 'irreversible' NMDA channel blocker MK-801 was used to tag synaptic receptors on cultured hippocampal neurons. Following MK-801 block of NMDA receptor-mediated EPSCs, there was an unexpected return of a substantial fraction ($\leq$40%) of the synaptic current over 5-7 minutes. The recovery could not be attributed to MK-801 unbinding or insertion of new receptors at synapses, suggesting that it was due to movement of receptors into the synapse. Using the reversible open-channel blocker ketamine, we found that as many as 65% of synaptic receptors were mobile. Our results provide additional evidence for a dynamic organization of receptors at central synapses.

Introduction

The anchoring of receptors opposite neurotransmitter release sites was initially taken as evidence of a stable postsynaptic membrane. This view was further strengthened with the identification of putative anchoring proteins such as rapsyn, gephyrin, and PSD-95 (Sanes and Lichtman, 1999; Kneussel and Betz, 2000; Sheng, 2001), and more recently with the wealth of recently discovered postsynaptic density (PSD) proteins and the concept of a molecular scaffold (Sheng, 2001). This molecular complexity would seem to suggest a relatively stable organization. At central excitatory synapses, the localization of receptors at relatively high density opposite neurotransmitter release sites is essential for high fidelity transmission given the low affinity of glutamate for α-amino-3-hydroxy-5-methyl-4-isoxazole-proprionic acid (AMPA) receptors (Patneau and Mayer, 1990). However recent evidence suggests that the presence of AMPA receptors at synapses is highly dynamic (Liu and Cull-Candy, 2000) such that these receptors can be rapidly shuttled between the synapse and intracellular compartments (Lüscher et al., 2000). Both the rapid incorporation of AMPA receptors into synapses and their removal by endocytosis is activity-dependent, suggesting that the shuttling may underlie several forms of synaptic plasticity (Beattie et al, 2000; Lüscher et al., 1999; Shi et al., 1999). The density of acetylcholine receptors at the neuromuscular junction also is activity-dependent (Akaaboune et al, 2000). In contrast, NMDA receptors, which are colocalized at synapses with AMPA receptors (Bekkers and Stevens, 1989; Jones and Baughman, 1991), appear to be fixed in the PSD complex (Moon et al., 1994; Lüscher et al, 1999).

The stability of receptors at synapses is generally addressed using biochemical or optical techniques. We examined whether NMDA are fixed at developing hippocampal synapses by taking advantage of the unique properties of 'irreversible' open-channel blocker (+)-MK-801(Huettner and Bean, 1988). Because MK-801 is a use-dependent antagonist, we used it as a high affinity label to tag synaptic NMDA receptors that opened in response to synaptically released glutamate. After binding to the receptor, MK-801 cannot dissociate unless the receptor rebinds ligand and reopens, thus repeated synaptic stimulation is predicted to irreversibly block NMDA-receptor meditated synaptic activity. However we found that there was a substantial

recovery of the NMDA-receptor mediated excitatory postsynaptic current (EPSC) after block of synaptic receptors. There was no recovery after block of all the NMDA receptors on the cell surface following whole-cell applications of NMDA and MK-801. Additional experiments with a low-affinity channel blocker, ketamine, suggested that the recovery represented bidirectional movement of receptors in and out of synapses. As many as 65% of NMDA receptors that bound synaptically released glutamate could be exchanged in < 7 minutes. Our data suggests that NMDA receptors are not fixed, but can be subject to ongoing exchange between synaptic and extrasynaptic pools.

Results

Anomalous Recovery from MK-801 block

NMDA receptor-mediated excitatory postsynaptic currents (EPSCs) were evoked in cultured autaptic hippocampal neurons (Bekkers an Stevens, 1991) at a holding potential of -70 mV. In the continuous presence of MK-801 during synaptic stimulation, the EPSC decay was accelerated and the amplitude was progressively reduced with repeated trials, consistent with an open-channel blocking mechanism (Fig 1A). Acceleration of the EPSC deactivation occurs because MK-801 block prevents reopenings later in the response. In 10 μM MK-801 the EPSC deactivation was significantly faster (τ_f=18.8 ± 1.4 msec; τ_s=133.7 ± 20.2 msec; Amp_f/Amp_s=2.64 ± 0.33; n=4) than control (τ_f=42.7 ± 1.2 msec: τ_s=310 ± 28.2 msec; Amp_f/Amp_s=1.07 ± 0.12; n=4). The 10-90% rise time in the presence of MK-801 (4.32 ± 0.17 msec; n=4) was also significantly faster than control (5.29 ± 0.23 msec; n=4), consistent with the shortening of the channel mean open time (Aldrich and Stevens, 1987). The peak amplitude of the first EPSC in the presence of MK-801 (10 μM) was 55 ± 1.5% of control (n=4). MK-801 failed to block EPSCs when it was co-applied with DL-AP5 (200 μM, n=6), indicating that MK-801 did not block closed channels.

Paired pulse stimuli were used to activate excitatory synapses. The NMDA component was measured after the decay of the AMPA component (Fig. 1B). NMDA receptors were blocked in two distinct ways. By whole-cell co-application of NMDA and MK-801, we should block all the receptors in the membrane. Alternatively, by applying MK-801 during synaptic stimulation, we

should selectively block synaptic receptors (Fig 1C, D, top). We defined a synaptic receptor as one that opens in response to synaptically released glutamate. Because MK-801 unbinds from NMDA receptors very slowly at –70 mV (Huettner and Bean, 1988), receptors that have bound MK-801 should no longer contribute to the NMDA receptor-mediated EPSC. We confirmed this by measuring EPSCs before and after whole-cell applications of NMDA (1 mM) and MK-801 (10-20 μM). Complete block of the agonist-evoked current was typically achieved with 4-5 co-applications (1 sec duration, 10-20 second interpulse interval, Fig 1C). EPSC acquisition was suspended during the NMDA and MK-801 co-application. The AMPA receptor-mediated EPSC was used to confirm that MK-801 block did not affect transmitter release. Because we used saturating NMDA concentrations, co-application of agonist and MK-801 should block all synaptic and extrasynaptic NMDA receptors. As expected, NMDA receptor-mediated EPSCs showed no recovery (-1.39 ± 2.3%, n=4), even 30 minutes after MK-801 removal (Fig 1C). In contrast, when synaptic receptors were selectively blocked, there was a consistent and significant recovery that reached 25-40%. To facilitate comparisons, we quantified the initial recovery at 50 stimuli (6.6 minutes) following removal of MK-801 (10.17 ± 2.86%, n=7, Fig 1D, 2C).

Recovery is consistent with incorporation of extrasynaptic receptors into synapses

The anomalous recovery of the NMDA receptor-mediated EPSC from selective MK-801 block of synaptic receptors could be accounted for by either of two broad possibilities. The recovery could simply reflect dissociation of MK-801 from NMDA receptors. Alternatively, the recovery could represent an increase in synaptic NMDA receptors, either through new synapse formation or an increased number of receptors at existing synapses. To investigate the first possibility, we tested for recovery from synaptic MK-801 block in the presence of a saturating concentration of a competitive NMDA receptor antagonist. The antagonist should prevent binding by NMDA receptors of synaptically released glutamate and thus channel opening of previously blocked channels. However, as shown in Figure 2A, DL-AP5 (200 μM) had no effect on the extent of recovery, as measured after removal of the antagonist (17.4 ± 7.95%, n=5, Fig 2D). Unbinding of MK-801 might also account for recovery if some synaptic NMDA receptors had a lower affinity for MK-801 (i.e. a faster unbinding rate). However, when the EPSC was allowed to

recover from selective MK-801 block of synaptic receptors, a co-application of NMDA and MK-801 produced a complete and irreversible block of the recovered EPSC (1.63 ± 1.22%, n=3; Fig 2B). Furthermore, EPSCs failed to recover from block by co-application of the lower affinity enantiomer (-)-MK-801 (5 μM) and NMDA (1 mM; data not shown). Thus, small differences in affinity could not be responsible for the observed recovery. MK-801 does not block desensitized receptors (Dzubay and Jahr, 1996). However, recovery could not be due to receptors leaving a long-lasting desensitized state because there was no recovery following whole-cell co-application of NMDA and MK-801. Thus we conclude that recovery must result from an increase in synaptic receptors.

An increase in synaptic receptors could occur due to insertion of new receptors into the membrane, recruitment of membrane receptors into existing synapses or creation of new synapses. However, the lack of recovery following whole-cell application of NMDA and MK-801 (Fig 1B) argues strongly against insertion of new receptors. We also did not see a gradual increase in the EPSC amplitude under control conditions, suggesting that there was not a net increase in synaptic sites containing NMDA receptors. This does not exclude the possibility that presynaptic terminals or active zones migrate to new areas of postsynaptic membrane, although this scenario would imply that extrasynaptic and synaptic membranes have relatively equal receptor densities. Because dendritic filopodia have been implicated in new synapse formation (Dailey and Smith, 1996; Ziv and Smith, 1996; Lendvai et al., 2000), we tested the effect of latrunculin B (2 μg/ml), a drug that arrests dendritic spine mobility (Fischer et al., 1998). Recovery was unaffected by latrunculin B (15.4 ± 2.3%, n=5; Fig 2C, 2D). The time course of recovery in our experiments was also more rapid than reported for assembly of new synapses in cultured hippocampal neurons (Friedman et al, 2000). Thus, it is unlikely that recruitment of surface receptors to new synapses accounts for the increase in the EPSC after MK-801 block. These data suggest that some NMDA receptors already in the membrane are initially far enough away from synaptically-released glutamate such that they are not blocked by MK-801 and EPSC recovery after MK-801 removal reflects movement of these receptors into the synapse.

Bidirectional movement of NMDA receptors at synapses

If receptors are continually moving into range of synaptically released glutamate, an open-channel blocker should continually and preferentially block the mobile receptors after the majority of the original synaptic receptors are blocked. In other words, receptors, as they enter the synapse, should continue to accumulate in the blocked state even after the EPSC is blocked. To test this prediction, we compared the fraction of tagged receptors on the entire cell with the fraction of synaptic receptors blocked as a function of stimulus number. We used the reversible open-channel blocker ketamine which acts similarly to MK-801 (Mayer et al., 1988), but has at least a 50-fold faster unbinding rate (MacDonald et al., 1991). As shown in Figures 3A and B, 10 stimuli in ketamine (50 μM) produced as much block of the EPSC as 30 stimuli (5.08±0.46% vs. 3.48±0.94% of control, n=24). To determine the fraction of ketamine-bound receptors ('tagged') in the membrane following block of the EPSC, we used a series of 5 depolarizing steps (+60 mV) in the presence of agonist to accelerate ketamine unbinding. Because ketamine unblock is use-dependent, the agonist-evoked current after several depolarizations was larger than the first agonist-evoked current (compare '1st' and '5th', Fig. 3C). The amplitude difference between the initial peak inward current in response to the 5th application and that of the first application represents the fraction of receptors on the cell tagged by ketamine. The fraction of receptors tagged by ketamine was much larger after 30 synaptic stimuli (10 stimuli: 16.9±2.0% of receptors in the membrane; 30 stimuli: 37.5±4.6% of receptors in the membrane, n=8, Fig 3D), indicating that additional receptors entered the synapse between stimuli 10 and 30. Receptors continued to accumulate at the synapse to a much greater degree than predicted from the progressive block of the EPSC (Fig. 3E). For this set of data, 42% of the receptors on the cell opened in response to synaptically released glutamate at some point during the experiment and 25% of the receptors on the entire cell entered a synapse within the 5 minutes between stimulus 10 and 50.

If some synaptic NMDA receptors are mobile, we might expect that they can move out of the synapse as well. We tagged synaptic receptors with ketamine and asked if they could move out of range of synaptically-released glutamate. As shown in Figure 4A, the NMDA receptor-mediated EPSC was completely blocked by ketamine (50 μM, 50 stimuli). Following ketamine removal, the EPSC amplitude gradually and fully recovered. The extent of recovery was

calculated by comparing the mean amplitude of 20 EPSCs immediately before ketamine application and 20 EPSCs after recovery from ketamine removal.

If synaptic receptors are fixed, full recovery of the EPSC means that there are no ketamine-blocked receptors on the cell. Following complete EPSC recovery, we used the agonist-evoked protocol to detect ketamine-tagged receptors (see Fig 3C). As before, the agonist-evoked current increased in a use-dependent way after several combined agonist applications and depolarizations, indicating the presence of tagged receptors (Fig. 4B). Our data indicates that 20.0±4.3% (n=6) of the receptors on the cell were ketamine-blocked, even after complete recovery of the EPSC. This represents the minimum fraction of receptors on the cell that moved out of the synapse. The same protocol in the absence of ketamine had no effect (2.0±3.1%, n=5, Fig 4C). These results indicate that a comparable number of NMDA receptors are moving into and out of the synapse over several minutes.

NMDA receptors at synapses preferentially contain the NR2A subunit whereas extrasynaptic receptors are largely composed of NR1/NR2B diheteromers (Tovar and Westbrook, 1999). We considered whether extrasynaptic receptors might be more mobile than synaptic receptors. However, the mobile fraction did not appear to be exclusively composed of NR1/2B diheteromers. If the fixed fraction was composed of NR2A-containing receptors and the mobile receptor fraction was composed of NR1/NR2B, the recovered EPSC after MK-801 block should be more sensitive to the NR1/NR2B-specific antagonist ifenprodil (Williams, 1993). Additionally, the EPSC deactivation from this recovered fraction should be slower because NR2A accelerates the EPSC deactivation (Vicini et al., 1998). However, the sensitivity of EPSCs to ifenprodil (3 μM) was not different before (43.5±3.4% of control) and after (40.9±4.1% of control) block by MK-801 (10-30 episodes, n=6). Likewise, the deactivation time constants before MK-801 (τ_f=39.7±2.2 msec, τ_s=267.7±11.6 msec; n=14) and after MK-801 (τ_f=36.0±2.7 msec, τ_s=239.2±9.4 msec) as well as the ratio of fast and slow components (1.22±0.13 before MK-801; 1.05±0.17 after MK-801) were similar.

We considered whether NMDA receptors consisted of a central fixed population surrounded by an annulus of mobile receptors. We reasoned that if the mobile fraction was further from the release site, these receptors would be exposed to lower glutamate concentrations. Thus, a low

affinity antagonist should preferentially block the mobile fraction (see Clements et al., 1992). However the sensitivity of the EPSC to low affinity competitive antagonists D-AA (30-60 μM) or L-AP5 (300-750 μM) was identical as measured before MK-801 and after most of the EPSC was blocked (data not shown). These data suggest that mobile and fixed receptor fractions experience similar glutamate concentration profiles and that when mobile receptors gate to synaptically-released glutamate, mobile and fixed receptors may be intermingled (see Clements, 1996).

Discussion

Our experiments were based on the ability to tag synaptic and total surface NMDA receptors with the open channel blockers, MK-801 and ketamine. A schematic summarizing our observations is shown in Figure 5. Selective tagging of the synaptic receptor complement ('synaptic block A') led to an accumulation of blocked receptors with repeated stimuli, some of which now resided in extrasynaptic membrane out of range of synaptically-released glutamate ('synaptic block B'). Upon washout of the blocker ('synaptic unblock'), the newly extrasynaptic receptors could only be unblocked if the cell was bathed in agonist ('agonist-evoked unblock') or a receptor moved back into range of synaptically released glutamate. Our data indicates that the synaptic complement of NMDA receptors is more dynamic than previously realized. Cycling of AMPA receptors has demonstrated that endocytosis and exocytosis may provide a mechanism for altering synaptic efficacy. The lateral movement of NMDA receptors between synaptic and extrasynaptic domains provides an alternate mechanism for altering synaptic strength in the time course of minutes.

The interpretation of recovery from MK-801 block as receptor mobility

We interpreted recovery of the synaptic response following selective MK-801 block of synaptic NMDA receptors as incorporation of unblocked receptors into pre-existing synapses. The most significant alternate explanations that must be considered are incorporation of new receptors from intracellular pools at synapses or formation of new synapses. The first possibility

is incompatible with the lack of recovery following MK-801 block of all surface NMDA receptors with whole-cell application. AMPA receptor incorporation at synapses has been shown to occur quickly following LTP induction protocols (Lüscher et al., 1999; Shi et al., 1999). However, this occurs only at a subset of synapses. If we assume that the turnover time of a synaptic NMDA is 16-24 hours (Huh and Wenthold, 1999), then after 0.5 hours (the average time of our experiments) only ≤2% of the receptors will be exchanged. Thus if receptor insertion occurred during the time course of our experiments, it did not contribute greatly to the EPSC recovery. In addition, the experiments with the low affinity blocker, ketamine provide strong evidence for bidirectional exchange of surface receptors between synaptic and extrasynaptic membrane. Receptor insertion could not account for the accumulation of ketamine-blocked receptors within the synapses the presence of tagged extrasynaptic receptors following selective synaptic stimulation.

Our evidence is also inconsistent with the possibility that recovery was due to the rapid formation of new synapses or active zones at the site of previously extrasynaptic NMDA receptors. The first argument here is a quantitative one. If movement of presynaptic active zones (Ahmari et al., 2000) accounted for recovery, there must be sufficient new sites to account for a 2-3 fold increase in synaptic NMDA receptors within 5 minutes (see figure 3E). That is, one must image a 3-fold increase in the number of synapses. Because all experiments were done using a constant stimulation protocol, then this predicts a marked increase in the EPSC amplitude during continuous recording in the absence of MK-801 or ketamine. This did not occur. The conclusion most consistent with our data is that a substantial fraction of the surface NMDA receptors are in dynamic motion. Thus the functional definition of synaptic receptors as those within range of synaptically released glutamate may not necessarily correspond to a synapse as defined by morphological clusters of receptors.

Lateral mobility of membrane proteins

The mobility of intrinsic plasma membrane proteins, including ion channels and ligand-gated receptors has been well investigated (Frye and Edidin, 1970; Young and Poo, 1983; Weiss et al., 1986). While proteins differ tremendously in their rates of diffusion (Weiss et al., 1986), the membrane diffusion coefficient of acetylcholine receptors (Young and Poo, 1983) indicates that a

receptor could diffuse across the PSD in ~1 second. While the NMDA receptor is larger, its free diffusion in a membrane should be much faster than the rate of movement predicted from our experiments. The difference between free diffusion presumably is related to interactions with anchoring and/or scaffolding proteins. These interactions are themselves dynamic and thus could influence apparent diffusion coefficients (Meier et al., 2001). Although a substantial number of NMDA receptors are extrasynaptic by physiological criteria (Tovar and Westbrook, 1999), these are difficult to quantify using immunohistochemical or optical methods. Given the small size of the PSD, it is likely that direct visualization of relatively local receptor movements, e.g. by recovery from photobleaching, may prove technically demanding.

Organization of the postsynaptic density

NMDA receptor subunits can remain tightly associated with the biochemically-purified PSD (see Kennedy, 1997). This implies that NMDA receptors can be bound within the postsynaptic complex. It is likely that tightly bound synaptic NMDA receptors are relatively immobile. Our experiments indicate that the fixed receptor fraction must be blocked during the first 10 stimuli because ketamine-blocked receptors accumulated after that point. Because 1/3 of the synaptic receptors were blocked in the first 10 stimuli, this means that at least ~65% of the synaptic receptors were mobile. Thus a significant fraction of NMDA receptors that respond to synaptically released glutamate were continually exchanged between synaptic and extrasynaptic domains.

The notion of mobile receptors is still consistent with a model of a highly organized postsynaptic membrane. Indeed, recent evidence has demonstrated that glycine receptors can exist in equilibrium between immobilized, gephyrin-associated states and mobile states (Meier et al., 2001). Our results do not resolve whether the mobility of NMDA receptors is regulated or reflects constitutive steady-state exchange between synaptic and extrasynaptic domains. Our experiments were done during a period of rapid synapse formation (6-9 days *in vitro*). While postsynaptic structures can be well visualized at this stage (Boyer et al., 1998) there are indications of a flexible synapse organization. For example, puncta of NMDA receptor subunit immunoreactivity have been reported on hippocampal neurons at a similar development stage,

but not all were colocalized with synaptic markers (Rao et al., 1998). Likewise, presynaptic release specializations in the absence of postsynaptic receptors have been demonstrated (Landis et al., 1989). Thus mobile NMDA receptors may be characteristic of newly formed excitatory synapses.

Given the highly ordered structure of the PSD, mobility of receptors into and out of the synapse may be a mechanism for receptor delivery or even use-dependent receptor removal (Heynen et al., 2000). For example, changes in the NMDA receptor phosphorylation resulting from receptor gating could increase the unbinding rate from anchoring proteins. These receptors could then leave the synapse and enter extrasynaptic domains where they could be endocytosed (Roche et al., 2000; Vissel et al., 2001). At the neuromuscular junction, receptors that leave the junction and are endocytosed (Akaaboune et al., 1999). Thus regulating the rates at which receptors can leave the synapse may lead to use-dependent modifications in the efficacy of synaptic transmission.

Conclusions

This work was an attempt to use the microculture system to describe some of the characteristics of nascent excitatory synapses. This work focused on synaptic NMDA receptors on cultured hippocampal neurons because of their presumed importance in the development of the nervous system. I took advantage of the culture system to study neurons from targeted-mutant mice, specifically ones that lack the NMDA receptor subunits NR2A, NR2B or both of the genes for these subunits. This would not be otherwise possible as mice lacking the NR2B subunit die soon after birth.

In this work I have shown that NR2A and NR2B are the only NR2 subunits expressed in these neurons. Excitatory postsynaptic currents (EPSCs) from neurons that lack NR2A have characteristics that are predicted from NR1/NR2B diheteromeric receptors. Similarly, EPSCs from neurons that lack the NR2B subunit have characteristics consistent with the expression of NR1/NR2A diheteromeric receptors. The decays of NMDA receptor-mediated EPSCs from these latter neurons are exceptionally fast and are not seen in wild-type cultured hippocampal neurons. Thus whenever NR2A is expressed, it is likely assembled into a triheteromeric receptor in combination with NR1 and NR2B. Neurons lacking both NR2A and NR2B had no NMDA-evoked currents and no NMDA receptor-mediated EPSCs but they did have AMPA-evoked currents and AMPA receptor-mediated EPSCs. This indicates that NMDA receptors are not required for synapse formation.

While the physiology from targeted mutant mice was mostly predicted from expression studies using *in situ* hybridization as well as Western blots, the wild-type developmental profile was not. As expected, the predominant receptors at nascent synapses were NR1/NR2B receptors, as judged by their ifenprodil sensitivity. However, fairly soon after synapses begin to form, a significant fraction of synaptic receptors contained the NR2A subunit, as determined by a decrease in ifenprodil sensitivity of the EPSC. Interestingly, in these same neurons, the extrasynaptic component appeared to be predominantly composed of NR1/NR2B receptors, as judged by their ifenprodil sensitivity. This indicates that there is a difference in distribution and/or targeting between diheteromeric NR1/NR2B receptors and triheteromeric

NR1/NR2A/NR2B receptors. Moreover, the lower ifenprodil sensitivity results from the existence of two distinct types of NMDA receptors at synapses. The characteristics of these are consistent with NR1/NR2B diheteromers and NR1/NR2A/NR2B triheteromeric receptors. This is the first demonstration that two types of NMDA receptors can exist in the postsynaptic membrane of a single neuron.

Finally, I found that a significant fraction of synaptic NMDA receptors are able to move between synaptic and extrasynaptic pools within minutes. While, post hoc, this is not a biologically surprising finding, it has been experimentally difficult to demonstrate and was only possible in this instance by the existence of high affinity NMDA open-channel blockers. Thus the density of synaptic NMDA receptors could be regulated by altering the binding or unbinding rates of NMDA receptors with their anchoring proteins or the density of extrasynaptic receptors. For example, the ratio of synaptic to extrasynaptic receptors decreases with time. Receptor mobility was a previously unappreciated regulatory mechanism.

The work in this thesis is a small inroad into the developmental phenomenology surrounding excitatory synapse formation. However, studies of synapses as they form are required in order to develop a complete model of self-organization of the nervous system.

References

Ahmari SE, Buchanan J, Smith SJ (2000) Assembly of presynaptic active zones from cytoplasmic transport packets. Nat Neurosci 3: 445-451.

Akaaboune M, Culican SM, Turney SG, Lichtman J. (2000). Rapid and reversible effects of activity on acetylcholine receptor density at the neuromuscular junction in vivo. Science 286: 503-507.

Aldrich RW, Stevens CF (1987). Voltage-dependent gating of single sodium channels from mammalian neuroblastoma cells. J. Neurosci. 7: 418-431.

Antonini A, Stryker MP (1993). Rapid remodelling of axonal arbors in the visual cortex. Science 260: 1819-1821.

Balice-Gordon R, Lichtman JW (1994). Long-term synapse loss induced by focal blockade of postsynaptic receptors. Nature 372: 519-524.

Bardoni R, Magherini PC, MacDermott AB (1998). NMDA EPSCs at glutamatergic synapses in the spinal cord of the postnatal rat. J Neurosci 18: 6558-6567.

Beattie EC, Carroll RC, Yu X, Morishita W, Yasunda H, von Zastrow M, Malenka RC (2000). Regulation of AMPA receptor endocytosis by a signaling mechanism shared with LTD. Nat Neurosci 3: 1291-1300.

Bekkers JM, Stevens CF (1989). NMDA and non-NMDA receptors are co-localized at individual excitatory synapses in cultured rat hippocampus. Nature 341: 230-233.

Bekkers JM, Stevens CF (1991). Excitatory and inhibitory autaptic currents in isolated hippocampal neurons maintained in cell culture. Proc Natl Acad Sci USA 88: 7834-7838.

Ben-Ari Y, Khazipov R, Leinekugel X, Caillard O, Gaiarsa JL (1997). $GABA_A$, NMDA and AMPA receptors: a developmentally regulated 'menage a trois'. Trends Neurosci 20: 523-529.

Bessho Y, Nawa H, Nakanishi S (1994). Selective up-regulation of an NMDA receptor subunit mRNA in cultured cerebellar granule cells by K+-induced depolarization and NMDA treatment. Neuron 12: 87-95.

Boyer C, Schikorski T, Stevens CF (1998). Comparison of hippocampal dendritic spines in culture and in brain. J Neurosci 18: 5294-5300.

Brenner HR and Sakmann B (1983). Neurotrophic control of channel properties at neuromuscular junction synapses of rat muscle. J Physiol (Lond) 337: 159-171.

Carmingnoto G, Vicini S (1992). Activity-dependent decreases in NMDA receptor responses during development of the visual cortex. Science 258: 1007-1011.

Chavis P, Westbrook G (2001) Integrins mediate functional pre- and postsynaptic maturation at a hippocampal synapse. Nature 411: 317-321.

Chen C, Okayama H (1987). High-efficiency transformation of mammalian cells by plasmid DNA. Mol Cell Biol 7: 2745-2752.

Chen CF, Regehr WG (2000). Developmental remodeling of the retinogeniculate synapse. Neuron 28: 955-966.

Cik M, Chazzot PL, Stephenson FA (1993). Optimal expression of cloned NMDAR1/NMDAR2A heteromeric glutamate receptors: a biochemical characterization. Biochem J 296: 877-883.

Clements JD, Lester RAJ, Tong G, Jahr CE, Westbrook GL (1992). The time course of glutamate in the synaptic cleft. Science 258: 1498-1501.

Clements JD (1996). Transmitter timecourse in the synaptic cleft: its role in central synaptic function. Trends Neurosci 19: 163-171.

Cline HT, Constantine-Paton M (1987). NMDA receptor antagonists disrupt the retinotectal topographic map. Neuron 3: 413-426.

Constantine-Paton M, Cline HT, Debski E (1990). Patterned activity, synaptic convergence, and the NMDA receptor in developing visual pathways. Annu Rev Neurosci 13: 129-154.

Constantine-Paton M, Cline HT (1998). LTP and activity-dependent synaptogenesis: the more alike they are, the more different they become. Curr Opin Neurobiol 8: 139-148.

Cottrell JR, Dube GR, Egles C, Liu G (2000). Distribution, density and clustering of functional glutamate receptors before and after synaptogenesis in hippocampal neurons. J Neurophysiol 84: 1573-1587.

Cull-Candy SG, Miledi R, Uchitel OD (1982). Properties of junctional and extrajunctional acetylycholine-receptor channels in organ cultured human muscle fibers. J Physiol (Lond) 333: 251-267.

Dailey ME, Smith SJ (1996). The dynamics of dendritic structure in developing hippocampal slices. J Neurosci 16: 2983-2994.

Dale HH, Feldberg W, Vogt M (1936). Release of acetylcholine at voluntary motor nerve endings. J Physiol 86: 353-380.

D'Angelo E, Rossi P, Taglietti V (1993). Different proportions of N-methyl-d-aspartate and non-N-methyl-d-aspartate receptor currents at the mossy fibre-granule cell synapse of developing rat cerebellum. Neuroscience 53: 121-130.

Das S, Sasaki YF, Rothe T, Premkumar LS, Takasu M, Crandall JE, Dikes P, Conner DA, Rayudu PV, Cheung W, Chen HS, Lipton SA, Nakanishi N (1998). Increased NMDA current and spine density in mice lacking the NMDA receptor subunit NR3A. Nature 393: 377-381.

Doupe AJ, Solis MM (1997). Song- and order-selective neurons develop in the songbird anterior forebrain during vocal learning. J Neurobiol 33: 694-709.

Durand GM, Kovalchuk Y, Konnerth A (1996). Long-term potentiation and functional synapse induction in developing hippocampus. Nature 381: 71-75.

Dzubay, J. A., and Jahr, C. E. (1996). Kinetics of NMDA channel opening. J Neurosci 16: 4129-4134.

Ebralidze AK, Rossi DJ, Tonegawa S, Slater NT (1996). Modification of NMDA receptor channels and synaptic transmission by targeted disruption of the NR2C gene. J Neurosci 15: 5014-5025.

Falls DL, Rosen KM, Corfas G, Lane WS, Fischbach GD (1993). ARIA, a protein that stimulates acetylcholine receptor synthesis, is a member of the neu ligand family. Cell 72: 801-815.

Feldman DE, Knudsen EI (1998). Experience-dependent plasticity and the maturation of glutamatergic synapses. Neuron 20: 1067-1071.

Fiala JC, Feinberg M, Popov V, Harris KM (1998). Synaptogenesis via dendritic filopodia in developing hippocampal area CA1. J Neurosci 18: 8900-8911.

Fischbach GD, Frank E, Jessell TM, Rubin LL, Schuetze SM (1979). Accumulation of acetylcholine receptors and acetylcholinesterase at newly formed nerve-muscle synapses. Pharmacol Rev 30: 411-428.

Fischbach GD and Rosen KM (1997). ARIA: a neuromuscular junction neuregulin. Annu Rev Neurosci 20: 429-458.

Fischer M, Kaech S, Knutti D, Matus A (1998). Rapid actin-based plasticity in dendritic spines. Neuron 20: 847-854.

Fletcher TL, De Camilli P, Banker G (1994). Synatogenesis in hippocampal cultures: evidence indicating that axons and dendrites become competent to form synapses at different stages of neuronal develoment. J Neurosci 14: 6695-6706.

Forrest D, Yuzaki M, Soares HD, Ng L, DC Luk, Sheng M, Stewart CL Morgan JI, Conner JA Curran T (1994) Targeted disruption of NMDA Receptor 1 gene abolishes NMDA response and results in neonatal death. Neuron 13: 325-338.

Fox K, Glazewski S, Schulze S (2000). Plasticity and stability of somatosensory maps in the thalamus and cortex. Curr Opin Neurobiol 20: 494-497

Frank E, Fischbach GD (1979). Early events in neuromuscular junction formation in vitro. J Cell Biol 83: 143-158.

Friedman HV, Bresler T, Garner CC, Ziv NE (2000). Assembly of new individual excitatory synapses: time course and temporal order of synaptic molecule recruitment. Neuron 27: 57-69.

Frye LD, Edidin M (1970). The rapid intermixing of cell surface antigens after formation of mouse-human heterokaryons. J. Cell Sci. 7: 319-335.

Gautam M, Noakes PG, Moscoso L, Rupp F, Scheller RH, Merlie JP, Sanes JR (1996). Defective neuromuscular synaptogenesis in agrin-deficient mutant mice. Cell 85:525-535.

Gomperts SN (1996). Clustering membrane proteins: it's all coming together with the PSD-95/SAP90 protein family. Cell 84: 659-662.

Gottmann K, Mehrle A, Gisselmann G, Hatt H (1997). Presynaptic control of subunit composition of NMDA receptors mediating synaptic plasticity. J Neurosci 17: 2766-2774.

Hessler NA, Shirke AM, Malinow R (1993). The probability of transmitter release at a mammalian central synapse. Nature 366: 569-572.

Hestrin S (1992). Developmental regulation of NMDA receptor-mediated synaptic currents at a central synapse. Nature 357: 686-689.

Heuttner JE, Bean BP (1988). Block of N-methyl-D-aspartate-activated current by the anticonvulsant MK-801: selective binding to open channels. PNAS 85: 1307-1311.

Heynen AJ, Quinlan EM, Bae DC, Bear MF (2000). Bidirectional activity-dependent regulation of glutamate receptors in the adult hippocampus in vivo. Neuron 28: 527-536.

Hohnke CD, Oray S, Sur M (2000). Activity-dependent patterning of retinogeniculate axons proceeds with a constant contribution from AMPA and NMDA receptors. J Neurosci 20: 8051-8060.

Hubel DH, Wiesel TN (1998). Early exploration of the visual cortex. Neuron 20: 401-12

Huh K-H, Wenthold RJ (1999). Turnover analysis of glutamate receptors identifies a rapidly degraded pool of the N-methyl-d-aspartate receptor subunit, NR1, in cultured cerebellar granule cell. J. Biol. Chem. 274: 151-157.

Isaac JT, Nicoll RA, Malenka RC (1995). Evidence for silent synapses: implications for the expression of LTP. Neuron 15: 427-434.

Isaac JT, Crair MC, Nicoll RA, Malenka RC (1997). Silent synapses during the development of thalamocortical inputs. Neuron 18: 269-280.

Jones KA and Baughman RW (1991). Both NMDA and non-NMDA subtypes of glutamate receptors are concentrated at synapses on cerebral cortical neurons in culture. Neuron 7: 593-603.

Katz B (1969). The release of neural transmitter substances. The Sherrington Lectures X. (Springfield, Illinois, USA: Charles C Thomas Publisher).

Kennedy MB (1997). The postsynaptic density at glutamatergic synapses. Trends Neurosci. 20: 264-268.

Kew JN, Richards JG, Mutel V, Kemp JA (1998). Developmental changes in NMDA receptor glycine affinity and ifenprodil sensitivity reveal three distinct populations of NMDA receptors in individual rat cortical neurons. J Neurosci 18: 1935-1943.

Kirson ED, Yaari Y (1996). Synaptic NMDA receptors in developing mouse hippocampal neurones: Functional properties and sensitivity to ifenprodil. J Physiol (Lond) 497: 437-455.

Kleinschimdt A, Bear MF, Singer W (1987). Blockade of NMDA receptors disrupts experience-dependent plasticity of kitten striate cortex. Science 238: 355-358.

Kneussel M, Betz H (2000). Clustering of inhibitory neurotransmitter receptors at developing postsynaptic sites: the membrane activation model. Trends Neurosci. 23: 429-435.

Kohr G and Seeburg PH (1996). Subtype-specific regulation of recombinant NMDA receptor-channels by protein tyrosine kinases of the src family. J Physiol (Lond) 492: 445-452.

Kornau H-C, Schenker LT, Kennedy MB, Seeburg PH (1995). Domain interactions between NMDA receptor subunits and the postsynaptic density protein PSD-95. Science 269: 1737-1740.

Krupp JJ, Vissel B, Heinemann SJ, Westbrook GL (1998). N-terminal domains in the NR2 subunit control desensitization of NMDA receptors. Neuron 20: 317-327.

Kutsuwada T, Kashiwabuchi N, Mori H, Sakimura K, Kushiya E, Araki K, Meguro H Masaki H, Kumanishi T, Arakawa M, Mishina M (1992). Molecular diversity of the NMDA receptor channel. Nature 358: 36-41.

Kutsuwada T, Sakimura K, Manabe T, Takayama C, Katakura N, Kushiya E, Natsume R, Watanabe M, Inoue Y, Yagi T, Aizawa S, Arakawa M, Takahashi T, Nakamura Y, Mori H, Mishina M (1996). Impairment of suckling response, trigeminal neuronal pattern formation, and hippocampal LTD in NMDA receptor ε2 subunit mutant mice. Neuron 16: 333-344.

Landis DM, Payne HR, and Weinstein LA (1989). Changes in the structure of synaptic junctions during climbing fiber synaptogenesis. Synapse 4: 281-293.

Laurie DJ, Putzke J, Zieglgansberger W, Seeburg PH (1995). The distribution of splice variants of the NMDAR1 subunit mRNA in the adult rat brain. Mol Brain Res 32: 94-108.

Legendre P and Westbrook GL (1991). Ifenprodil blocks N-methyl-D-aspartate receptors by a two-component mechanism. Mol Pharm 40: 289-298.

Legendre P, Rosenmund C, Westbrook GL (1993). Inactivation of NMDA channels in cultured hippocampal neurons by intracellular calcium. J Neurosci 13: 674-684.

Lendvai B, Stern EA, Chen B, Svoboda K (2000). Experience-dependent plasticity of dendritic spines in the developing rat barrel cortex in vivo. Nature 404: 876-881.

Li JH, Wang YH, Wolfe BB, Krueger KE, Corsi L, Stocca G, Vicini S (1998). Developmental changes in localization of NMDA receptor subunits in primary cultures of cortical neurons. Eur J Neurosci 10: 1704-1715.

Li Y, Erzurumlu RS, Chen C, Jhaveri S, Tonegawa S (1994). Whisker-related neuronal patterns fail to develop in the trigeminal brainstem nuclei of NMDAR1 knockout mice. Cell 76: 427-437.

Liao D, Hessler NA, Malinow R (1995). Activation of postsynaptically silent synapses during pairing-induced LTP in CA1 region of hippocampal slice. Nature 375: 400-404.

Lichtman JW, Colman H (2000). Synapse elimination and indelible memory. Neuron 25: 269-278.

Lin W, Burgess RW, Dominguez B, Pfaff SL, Sanes JR, Lee K-F (2001). Distinct roles of nerve and muscle in postsynaptic differentiation of the neuromuscular synapse. Nature 410: 1057-1064.

Lindlbauer R, Mohrmann R, Hatt H, Gottmann K (1998). Regulation of kinetic and pharmacological properties of synaptic NMDA receptors depends on presynaptic exocytosis in rat hippocampal neurons. J Physiol (Lond) 508: 495-502.

Liu S-QJ and Cull-Candy SG (2000). Synaptic activity at calcium-permeable AMPA receptors induces a switch in receptor subtype. Nature 405: 454-458.

Luscher C, Xia H, Beattie EC, Carroll RC, von Rastrow M, Malenka RC, Nicoll RA (1999). Role of AMPA receptor cycling in synaptic transmission and plasticity. Neuron 24: 649-658.

MacDonald JF, Bartlett MC, Mody I, Pahapill P, Reynolds JN, Salter MW, Schneiderman JH, Pennefather PS (1991). Actions of ketamine, phencyclidine and MK-801 on NMDA receptor currents in cultured mouse hippocampal neurones. J Physiol (Lond) 432: 483-508.

Martinou JC, Falls DL, Fischbach GD (1991). Acetylcholine receptor-inducing activity stimulates expression of the e-subunit gene of the muscle acetylcholine receptor. Proc Natl Acad Sci, USA 88: 7669-7673.

Mayer ML, Westbrook GL, Guthrie PB (1984) Voltage-dependent block by Mg2+ of NMDA responses in spinal cord neurones. Nature 309: 261-263.

Mayer ML, Westbrook, GL, Vyklicky Jr L. (1988). Sites of antagonist action on N-methyl-D-aspartic acid receptors: studies using fluctuation analysis and a rapid perfusion technique. J Neurophysiol 60: 645-663.

McBain CJ, Mayer ML (1994). NMDA receptor structure and function. Physiol Rev 74: 723-760.

McDonald JW, Johnston MV (1990). Physiological and pathophysiological roles and excitatory amino acids during central nervous system development. Brain Res Rev 15: 41-70.

Meier J, Vannier C, Serge A, Triller A, Choquet D (2001) Fast and reversible trapping of surface receptors by gephyrin. Nat Neurosci. 4: 253-260.

Monyer H, Burnashev N, Laurie DJ, Sakmann B, Seeburg PH (1994). Developmental and regional expression in the rat brain and functional properties of four NMDA receptors. Neuron 12: 529-540.

Mori H, Manabe T, Watanabe M, Satoh Y, Suzuki N, Toki S, Nakamura K, Yagi T, Kushiya E, Takahashi T, Inoue Y, Sakimura K, Mishina M (1998). Role of the carboxy-terminal region of the GluR ε2 subunit in synaptic localization of the NMDA receptor channel. Neuron 21: 571-580.

Moon IL, Apperson ML, Kennedy MB (1994). The major tyrosine-phosphorylated protein in the postsynaptic density fraction is N-methyl-D-aspartate receptor subunit 2B. Proc Natl Acad Sci U.S.A. 91: 3954-3958.

Nowak L, Bregestovski, Ascher P, Herbet A, Prochiantz A (1984). Magnesium gates glutamate-activated channels in mouse central neurones. Nature 307: 462-465.

Orser BA, Pennefather PS, MacDonald JF (1997). Multiple mechanisms of ketamine blockade of N-methyl-D-aspartate receptors. Anesthesiology 86: 903-917.

Ozaki M, Sasner M, Yano R, Lu HS, Buonanno A (1997). Neuregulin-β induces expression of an NMDA-receptor subunit. Nature 390: 691-694.

Paoletti P, Ascher P, Neyton J (1997). High-affinity zinc inhibition of NMDA NR1-NR2A receptors. J Neurosci 17: 5711-5725.

Patneau DK, Mayer ML (1990). Structure-activity relationships for amino acid transmitter candidates acting at N-methyl-D-aspartate and quisqualate receptors. J Neurosci 10: 2385- 2399.

Plant T, Schirra C, Garaschuk O, Rossier J, Konnerth A (1997). Molecular determinants of NMDA receptor function in GABAergic neurones of rat forebrain. J Physiol (Lond) 499: 47-63.

Rao A, Craig AM (1998). Activity regulates the synaptic localization of the NMDA receptor in hippocampal neurons. Neuron 19: 801-812.

Rao A, Kim E, Sheng M, Craig AM (1998). Heterogeneity in the molecular composition of excitatory postsynaptic sites during development of hippocampal neurons in culture. J Neurosci 18: 1217-1229.

Reist NE, Werle MJ, McMahan UJ (1992). Agrin released by motor neurons induces the aggregation of acetylcholine receptors at neuromuscular junctions. Neuron 8: 865-868

Roche KW, Standley S, McCallum J, Ly CD, Wenthold RJ (2001). NMDA receptor internalization is regulated by PSD-95. J. Neurosci. Abst. 30.

Rosenmund C, Clements JD Westbrook GL (1993). Nonuniform probability of glutamate release at a hippocampal synapse. Science 262: 754-757.

Rosenmund C, Feltz A, Westbrook GL (1995). Synaptic NMDA receptor channels have a low open probability. J Neurosci 15: 2788-2795.

Sah P, Hestrin S, Nicoll RA (1989). Tonic activation of NMDA receptors by ambient glutamate enhances excitability of neurons. Science 246: 815-818.

Sakimura K, Kutsuwada T, Ito I, Manabe T, Takayama C, Kushiya E, Yagi T, Aizawa S, Inoue Y, Sugiyama H, Mishina M (1995). Reduced hippocampal LTP and spatial learning in mice lacking NMDA receptor ε1 subunit. Nature 373: 151-155.

Sanes JR, Lawrence JC Jr (1983). Activity-dependent accumulation of basal lamina by cultured rat myotubes. Dev Biol 97: 123-136.

Sanes JR, Lichtman JW (1999). Development of the vertebrate neuromuscular junction. Annu Rev Neurosci 22: 389-442.

Segal EE, Furshpan EJ (1990). Epileptiform activity in microcultures containing small numbers of hippocampal neurons. J Neurophysiol 64: 1390-1399.

Shatz CJ (1990). Impulse activity and the patterning of CNS connections during development. Neuron 5: 745-756.

Sheetz AJ, Constantine-Paton M (1994). Modulation of NMDA receptor function: implications for vertebrate neural development. FASEB J 8: 745-752.

Sheng M, Cummings J, Roldan LA, Jan YN, Jan LY (1994). Changing subunit composition of heteromeric NMDA receptors during development in rat cortex. Nature 368: 144-147.

Sheng M, Wyszynski M (1997). Ion channel targeting in neurons. Bioassays 19: 847-853.

Sheng MH-T (2001). The postsynaptic specialization. In Synapses, WM Cowan, TC Sudhof, CF Stevens eds. (Baltimore, MD: The Johns Hopkins University Press), pp. 315-355.

Shi, S. H. Hayashi, Y., Petralia, R. S., Zaman, S. H., Wenthold, R. J., Svoboda, K. and Malinow, R. (1999). Rapid spine delivery and redistribution of AMPA receptors after synaptic NMDA receptor activation. Science 284: 1811-1816.

Sprengel R, Suchanek B Amico C, Brusa R, Burnashev N, Rozov A, Hvalby O Jensen V, Paulsen O, Andersen P, Kim JJ, Thompson RF, Sun W, Webster LC, Grant SG, Eilers J, Konnerth A, Li J, McNamara JO, Seeburg PH (1998). Importance of the intracellular domain of NR2 subunits for NMDA receptor function *in vivo*. Cell 92: 279-289.

Stent GS (1973). A physiological mechanism for Hebb's postulate of learning. Proc Natl Acad Sci USA 70: 997-1001.

Stocca G and Vicini S (1998). Increased contribution of NR2A subunit to synaptic NMDA receptors in developing rat cortical neurons. J Physiol 507: 13-24.

Tong G, and Jahr CE (1994) Multivescicular release from excitatory synapses of cultured hippocampal neurons. Neuron 12: 51-59.

Tong G, Shepherd D, and Jahr CE (1995). Synaptic desensitization of NMDA receptors by calcineurin. Science 267: 1510-1512.

Tovar KR, Miller AJ and Westbrook GL (1998). The ε2 NMDA receptor subunit is not required for synaptic clustering of NMDA receptors. Soc Neurosci Abstract 24:90.

Tovar KR and Westbrook GL (1999). The incorporation of NMDA receptors with a distinct subunit composition at nascent hippocampal synapses *in vitro*. J Neurosci 19: 4180-4188.

Vicini S, Wang J, Li J, Zhu W, Wang Y, Luo J, Wolfe B, and Grayson D (1998). Functional and pharmacological differences between recombinant N-methyl-D-aspartate receptors. J Neurophysiol 79: 555-566.

Vissel B, Krupp JJ, Heinemann SF, Westbrook GL (2001). A use-dependent tyrosine dephosphorylation of NMDA receptors is independent of ion flux. Nat. Neurosci. in revision.

Washburn MS, Numberger M, Zhang S, Dingledine R (1997) Differential dependence on GluR2 expression of three characteristic features of AMPA receptors. J Neurosci 17: 9393-9406

Weiss RE, Roberts WM, Stühmer W, and Almers W (1986). Mobility of voltage-dependent ion channels and lectin receptors in the sarcolemma of frog skeletal muscle. J. Gen. Physiol. 87: 955-983.

Westerfield M, Liu DW, Kimmel CB, Walker C (1990). Pathfinding and synapse formation in a zebrafish mutant lacking functional acetylcholine receptors. Neuron 4: 867-874.

Williams K (1993). Ifenprodil discriminates subtypes of the N-methyl-D-aspartate receptor: selectivity and mechanisms at recombinant heteromeric receptors. Mol Pharm 44: 851-859.

Wong RO, Oakley DM (1996). Changing patterns of spontaneous bursting activity of on and off retinal ganglion cells during development. Neuron 16: 1087-1095.

Wong RO (1999). Retinal waves and visual development. Annu Rev Neurosci 22:29-47.

Wong WT, Faulkner-Jones BE, Sanes JR, Wong RO (2000). Rapid dendritic remodeling in the developing retina: dependence on neurotrasmission and reciprocal regulation by Rac and Rho. J Neurosci 20: 5024-5036.

Wu GY, Malinow R, Cline HT (1996). Maturation of a central glutamatergic synapse. Science 274: 972-976.

Wyszynski M, Lin J, Rao A, Nigh E, Beggs AH, Craig AM, Sheng M (1997). Competitive binding of α-actinin and calmodulin to the NMDA receptor. Nature 385: 439-442.

Young, S. H. and Poo, M. M. (1983). Rapid lateral diffusion of extrajunctional acetylcholine receptors in the developing muscle membrane of *Xenopus* tadpole. J. Neurosci. 3: 225-231.

Zhong J, Russell SL, Pritchett DB, Molinoff PB, Williams K (1994). Expression of mRNAs encoding subunits of the N-methyl-d-aspartate receptor in cultured cortical neurons. Mol Pharm 45: 846-853.

Ziff EB (1997). Enlightening the postsynaptic density. Neuron 19: 1163-1174

Ziv NE and Smith SJ (1996). Evidence for a role of dendritic filopodia in synaptogenesis and spine formation. Neuron 17: 91-102.

Illustrations

Figure 1

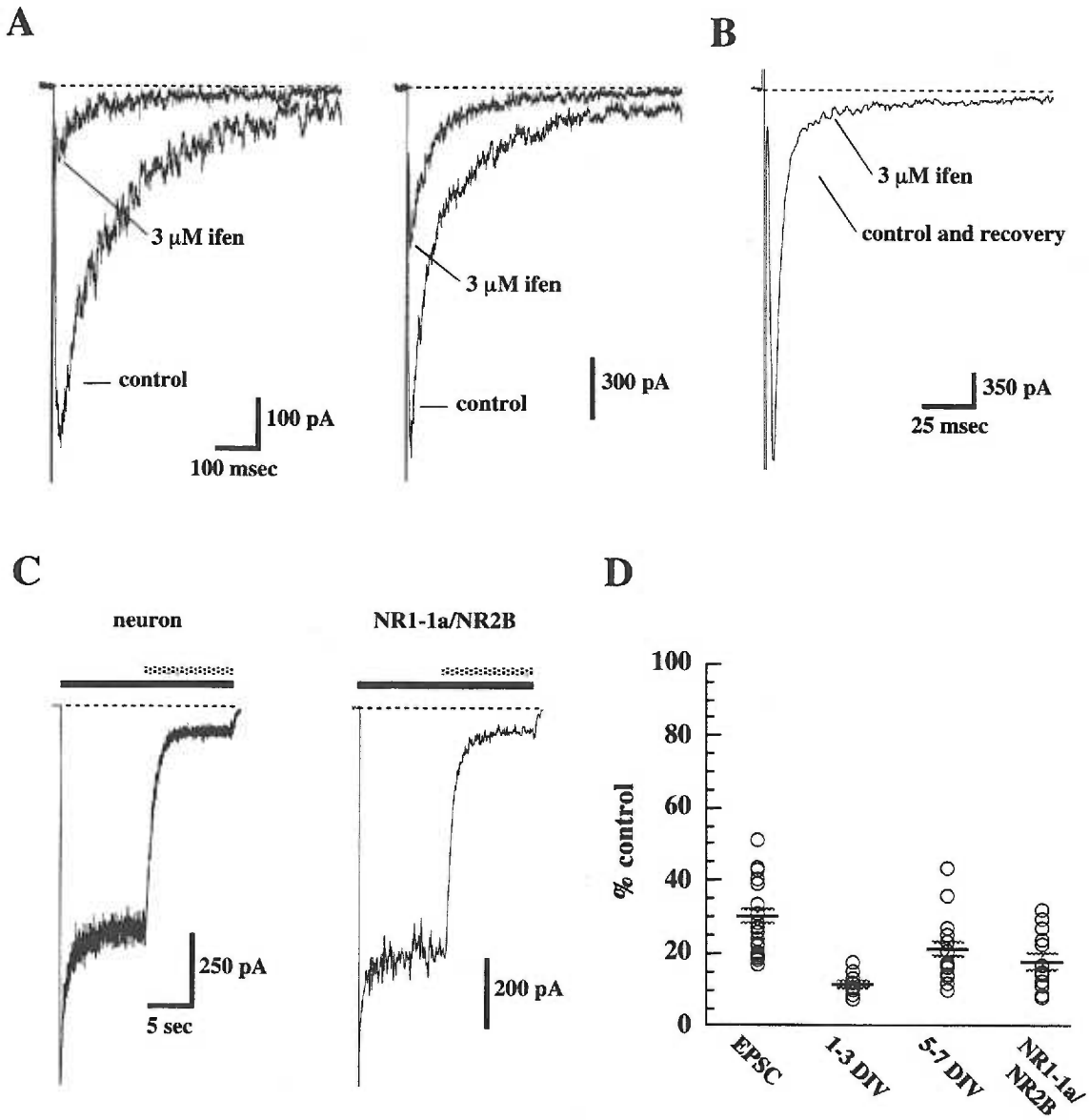

Figure 1.

Ifenprodil blocks NMDA EPSCs and whole-cell currents. *A*, NMDA EPSCs (in 5 μM CNQX) from neurons at 5 (left) and 7 DIV, in control solution or with 3 μM ifenprodil, plotted on the same time scale, showing the heterogeneity of ifenprodil's antagonism. *B*, EPSC showing both AMPA (fast) and NMDA (slow) components of the EPSC. The fast component is unaffected by 3 μM ifenprodil. *C*, Ifenprodil block of whole-cell currents in neurons and HEK293 cells transfected with NR1-1a and NR2B is similar. In 1 mM NMDA, applications of 3 μM ifenprodil were made to neurons (left) or transfected cells (right) once the control currents reached steady-state. Currents are plotted on the same time scale. Bars above the currents represent NMDA (solid black) and ifenprodil (gray) applications. *D*, Scatter plot of ifenprodil block of EPSCs and whole-cell currents from neurons at ≤7 DIV plotted with whole-cell data from HEK293 cells, for comparison. Solid bars represent the group mean.

Figure 2

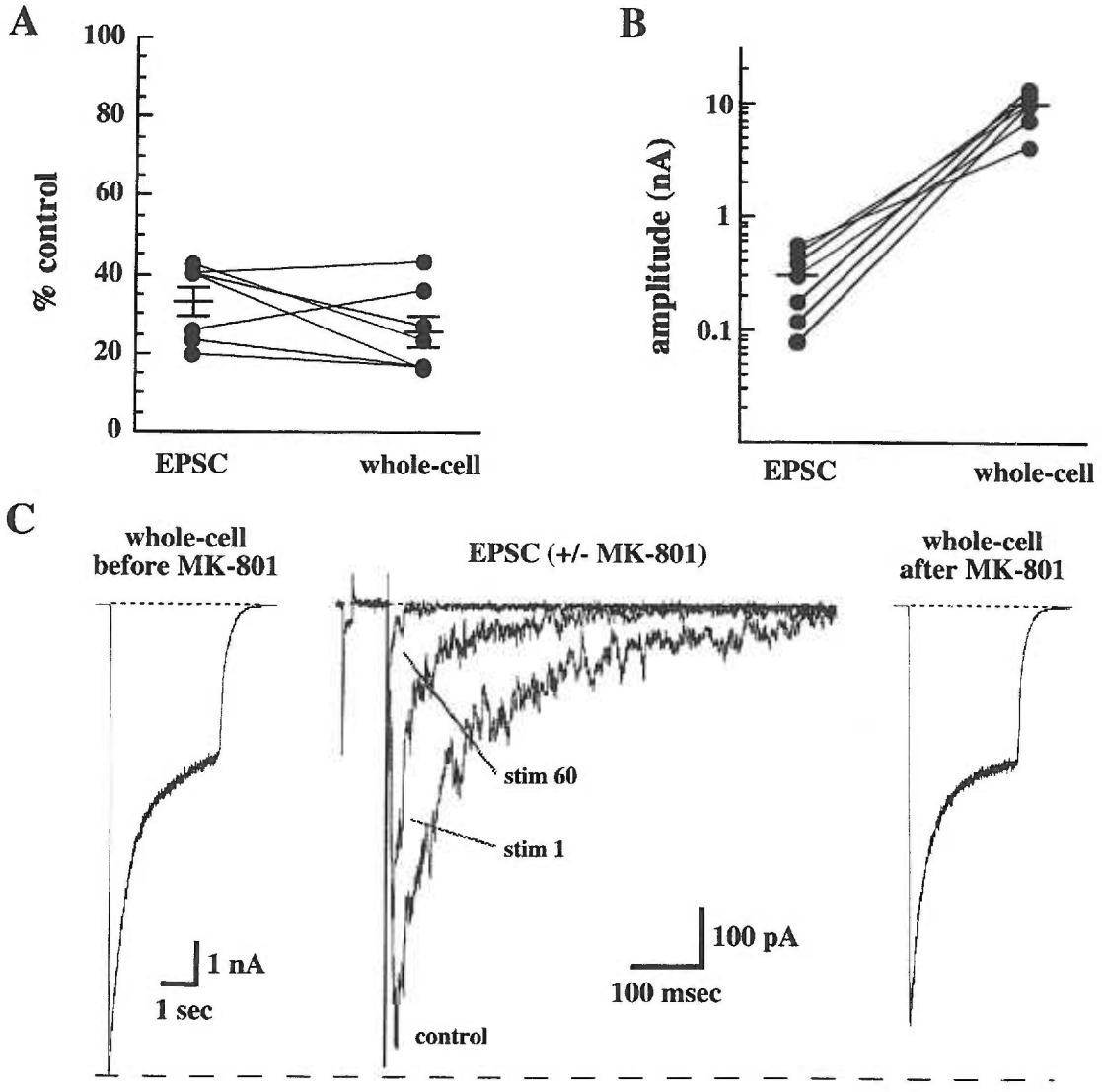
A
100
80
60
40
20
0
% control
EPSC
whole-cell
B
10
1
0.1
amplitude (nA)
EPSC
whole-cell
C
whole-cell
before MK-801
EPSC (+/- MK-801)
whole-cell
after MK-801
stim 60
stim 1
1 nA
1 sec
100 pA
100 msec
control

Figure 2.

Extrasynaptic NMDA receptors outnumber synaptic receptors by 3:1 in ≤7 DIV neurons. *A*, Ifenprodil sensitivity of EPSCs and whole-cell currents measured in the same neurons. Gray lines indicate the corresponding paired currents from individual neurons. *B*, shows a scatter plot comparison of peak EPSC and whole-cell current amplitudes from the cells in *A*. In doing a pair-wise comparison, the mean fold-difference between EPSC and whole-cell current amplitudes was 55.6 ± 17.7. C, shows the experimental approach used to eliminate synaptic receptors from the whole-cell current. The first current is the whole-cell response to 1 mM NMDA before any experimental manipulation. The next currents show NMDA EPSCs in control and in 5 μM MK-801 (1st and 60th stimuli shown). By the 60th stimulus, >95% of the EPSC has been blocked. Once EPSCs were blocked another whole-cell application of 1 mM NMDA was made, as shown in the final current. The difference between the peak in the first current and the last current reflect the proportion of NMDA receptors at synapses. EPSCs were stimulated at 0.1 Hz.

Figure 3

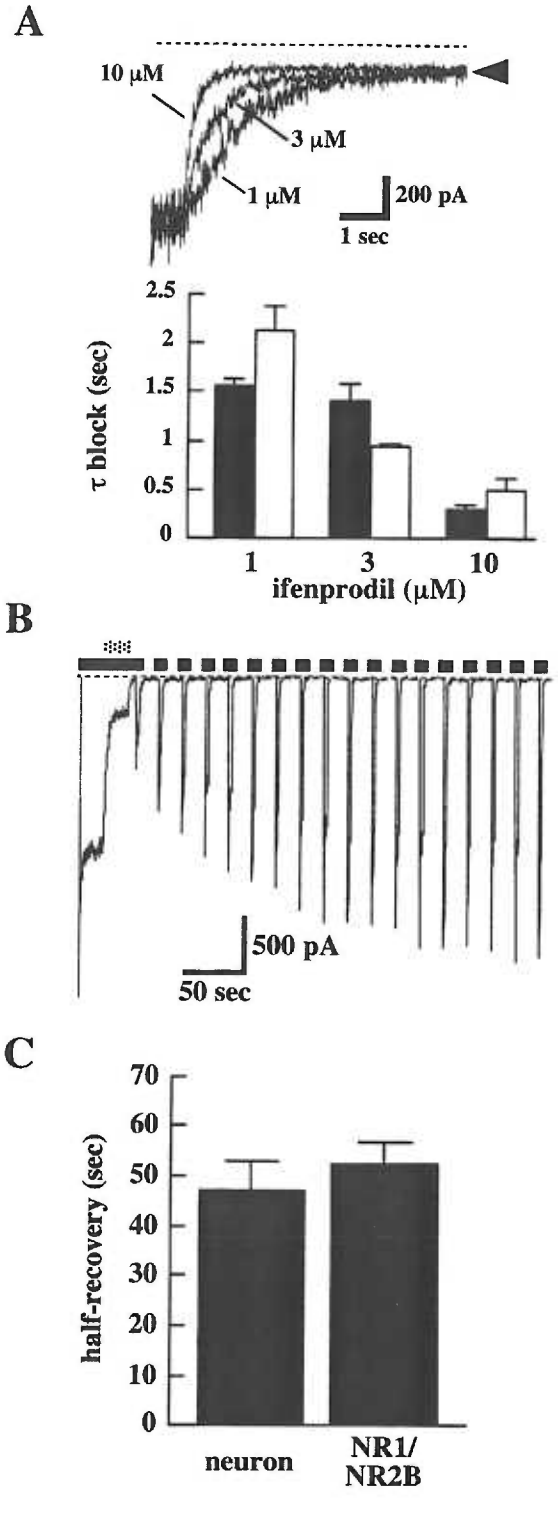
A
10 μM
3 μM
1 μM
200 pA
1 sec
τ block (sec)
2.5
2
1.5
1
0.5
0
1
3
10
ifenprodil (μM)
B
500 pA
50 sec
C
half-recovery (sec)
70
60
50
40
30
20
10
0
neuron
NR1/
NR2B

Figure 3.

Macroscopic kinetic properties of NMDA receptors in ≤7 DIV neurons and recombinant NR1/NR2B receptors are similar. *A*, Detail of relaxations in 1, 3 and 10 μM ifenprodil, as indicated. The arrowhead indicates that the steady-state amplitude reduction is approximately the same for these three concentrations. The relaxations were fit with single exponentials and the results were plotted below the raw data in *A*. *B*, shows the protocol for measuring the recovery from ifenprodil block of whole-cell currents. This example is from a neuron at 6 DIV. Bars above the current are as in Fig 1C. *C*, bar graphs of half-recovery times using the protocol shown in *B*, showing the similarity in the recovery from block between native NMDA receptors at ≤7 DIV and recombinant NR1/NR2B receptors.

Figure 4

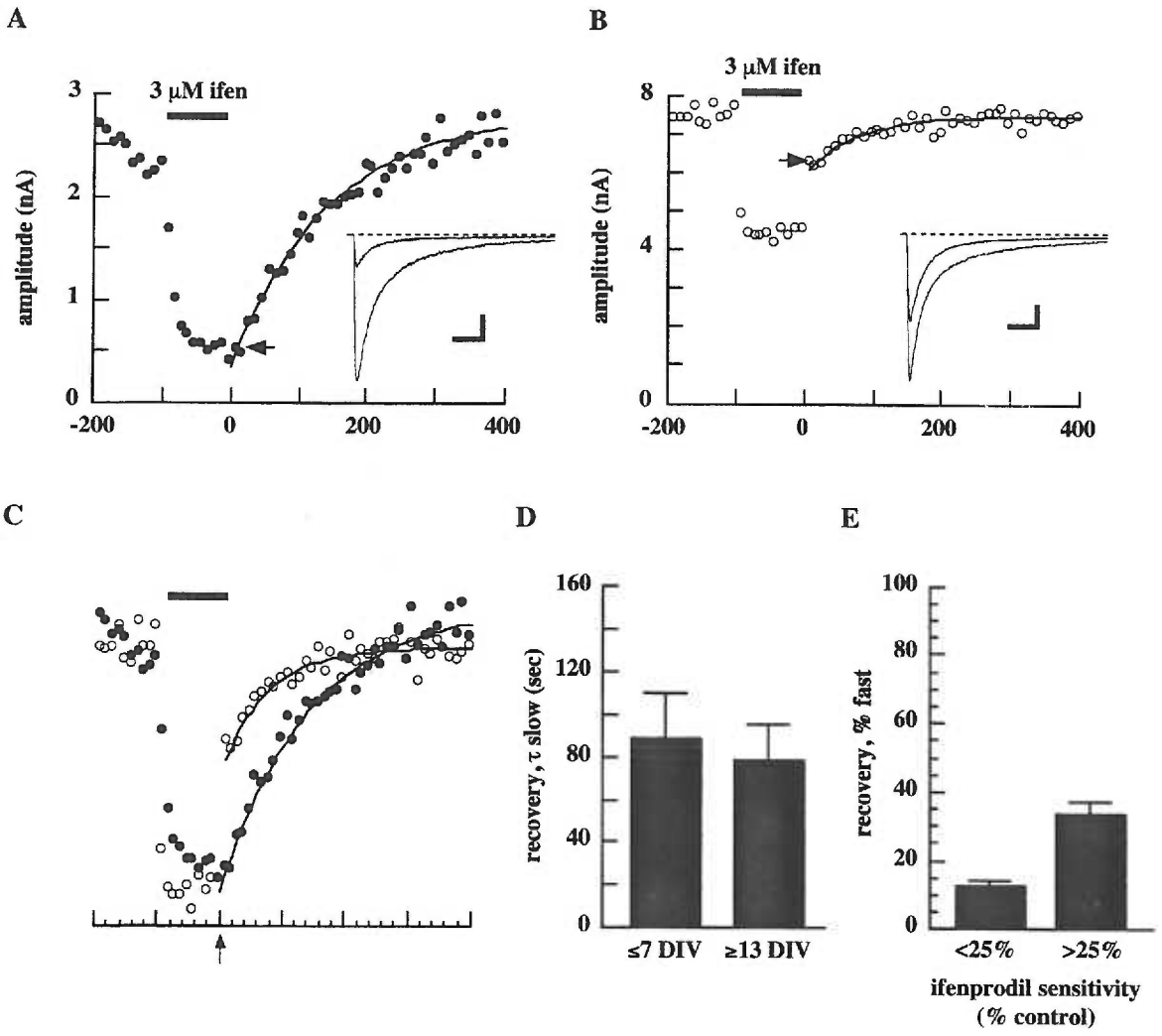
A
3 μM ifen
amplitude (nA)
3
2
1
0
-200
0
200
400
B
3 μM ifen
amplitude (nA)
8
4
0
-200
0
200
400
C
D
recovery, τ slow (sec)
160
120
80
40
0
≤7 DIV
≥13 DIV
E
recovery, % fast
100
80
60
40
20
0
<25%
>25%
ifenprodil sensitivity
(% control)

Figure 4.

Synaptic NMDA receptor complement can be composed of two distinct types of NMDA receptors. *A*, Plot of peak NMDA EPSC amplitude as a function of recording time from a neuron at 7 DIV. The plot represents the amplitude of the last 10 EPSCs before the 3 μM ifenprodil application followed by the amplitude of 10 EPSCs in ifenprodil. The solid bar represents the ifenprodil application. The arrowhead points to the first EPSC after ifenprodil removal. *B*, as in *A* except from a neuron at 15 DIV. In *A* and *B*, the insets show EPSCs in control and in 3 μM ifenprodil. Scale: 400 pA and 1 nA, respectively, and 100 msec for both. Note that in this example the first EPSC after ifenprodil removal had recovered more than half of the total extent of block in the 10 second interval between EPSCs (arrowhead). Stimulus frequency is 0.1 Hz and current amplitudes were measured with a 5 millisecond window around the peak. Ifenprodil was applied with a flowpipe positioned 50-100 μm from the soma. In both cases the recovery from block was fitted with a single exponential starting at the first data point after ifenprodil removal. *C*, shows the normalized plots from *A* and *B* to show the extent of recovery after ifenprodil removal. The arrow indicates the last EPSC in ifenprodil. *D*, compares the slow recovery time constants of EPSCs from ≤7 DIV and ≥13 DIV neurons. *E*, shows that EPSCs that were more sensitive to block by ifenprodil recovered less in the first interval after ifenprodil removal than that EPSCs that were less sensitive to ifenprodil block.

Figure 5

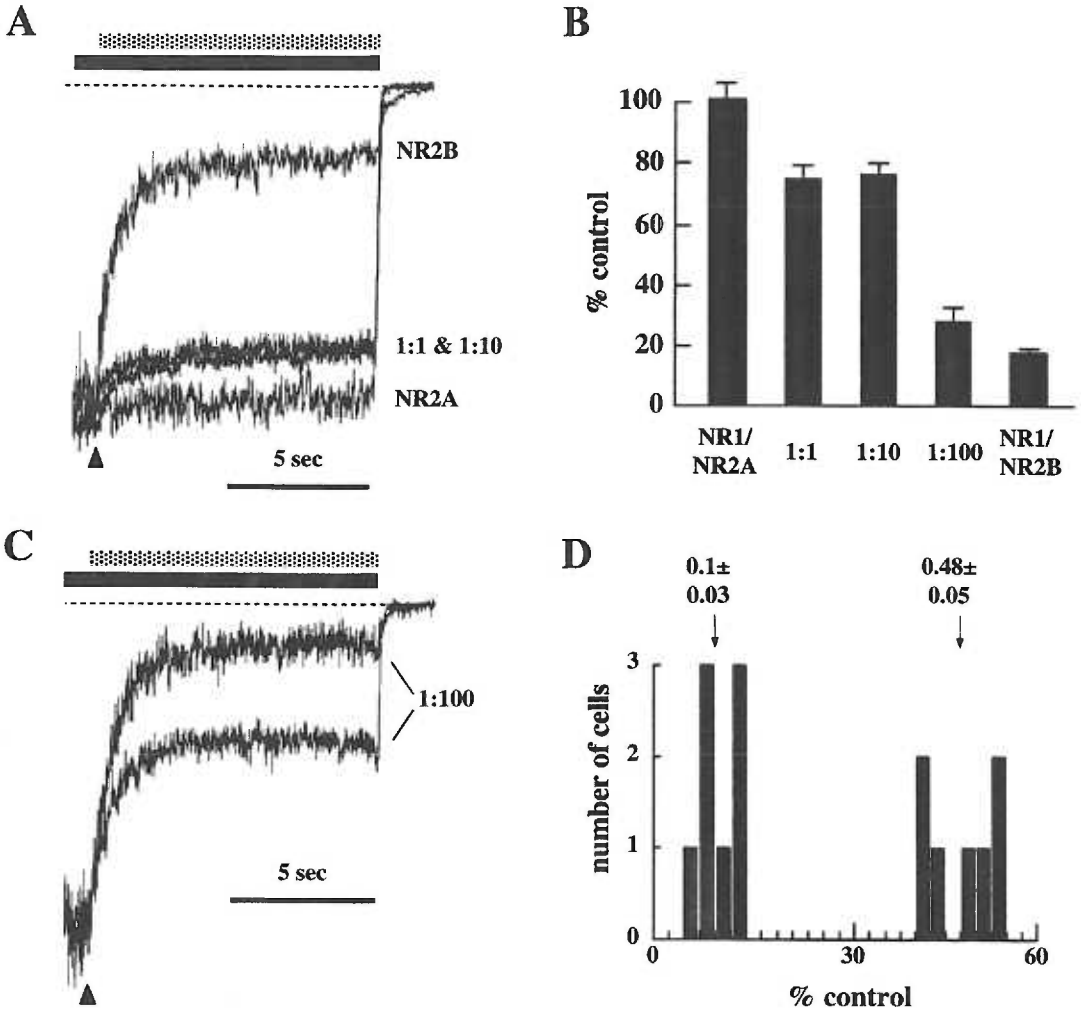
A
NR2B
1:1 & 1:10
NR2A
5 sec
B
100
80
60
40
20
0
% control
NR1/
NR2A
1:1
1:10
1:100
NR1/
NR2B
C
1:100
5 sec
D
0.1±
0.03
0.48±
0.05
3
2
1
0
number of cells
0
30
60
% control

Figure 5.

High ifenprodil sensitivity is a property of NR1/NR2B receptors. HEK293 cells were transfected with varying ratios of NR2A and NR2B subunit, as well as with NR2A or NR2B alone. *A*, shows whole-cell current relaxations in ifenprodil from HEK293 cells transfected with (from the top) NR1/NR2B; NR1/NR2A:NR2B; NR1/NR2A:10NR2B (overlapping) or NR1/NR2A alone. *B*, shows plots of all the data from these experiments. *C*, shows the two groups of responses from the 1:100 NR2A:NR2B transfections. *D*, shows the distribution of ifenprodil sensitivity from the group transfected with 1:100 NR2A:NR2B. Bars above the currents in *A* and *C* are as in Fig 1C. Data in *A* and *C* were normalized to the start of ifenprodil application (as indicated by arrowhead).

Figure 6

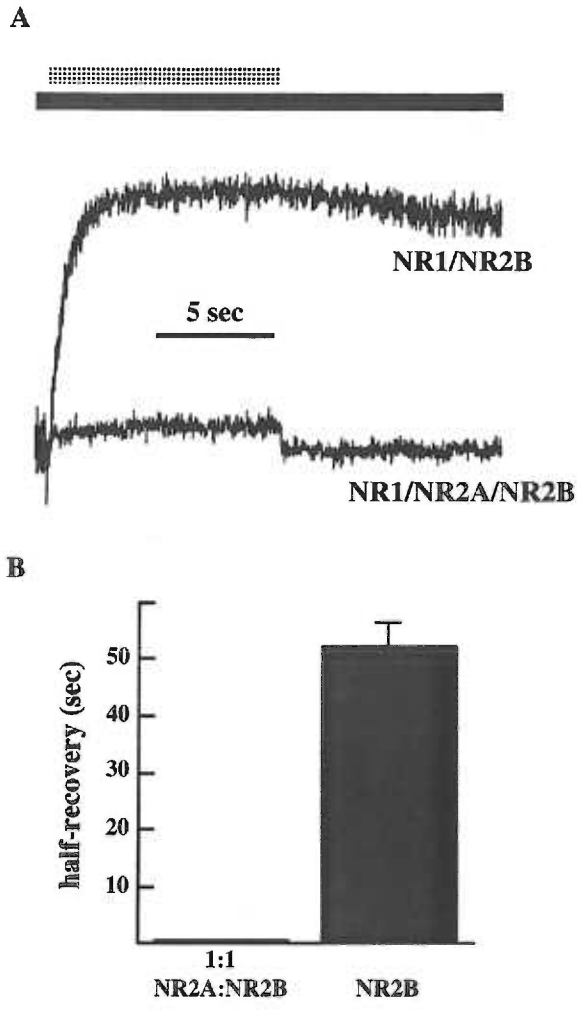
A
NR1/NR2B
5 sec
NR1/NR2A/NR2B
B
half-recovery (sec)
50
40
30
20
10
1:1
NR2A:NR2B
NR2B

Figure 6.

HEK293 cells transfected with NR1, NR2A and NR2B recovery quickly from ifenprodil block. *A*, shows the protocol for measuring the recovery from block from triply-transfected cells (with a 1:1 ratio of NR2A to NR2B) and the recovery from block of a NR1/NR2B-transfected cell for comparison. Data for block recovery is shown in *B*. Recovery data for NR1/NR2B cells is reiterated from figure 3C and collected using the method illustrated in 3B. This method could not be used for triply-transfected cells since often the recovery was completed in the interval between the removal of ifenprodil and the first application of NMDA alone. Instead, recovery was measured by returning to the NMDA solution lacking ifenprodil. An example using this method of measuring recovery from block from NR1/NR2B receptors is shown for comparison. Bars above the current are as in Fig 1C.

Figure 7

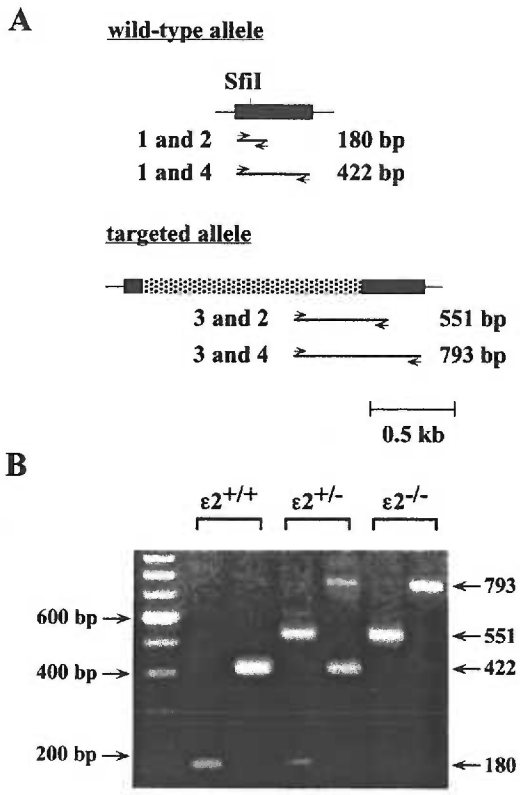
A
wild-type allele
SfiI
1 and 2
180 bp
1 and 4
422 bp
targeted allele
3 and 2
551 bp
3 and 4
793 bp
0.5 kb
B
ε2+/+
ε2+/-
ε2-/-
600 bp
400 bp
200 bp
793
551
422
180

Figure 7.

Genotyping of ε2-targeted mice. Mice were genotyped using the polymerase chain reaction (PCR), allowing determination of the genotype of the animal within 2-3 days after plating. Two separate reactions were used for each genomic DNA sample. Primer orientation and placement is shown in *A*. The reactions differed only in the primers used (see methods). Because each reaction amplifies a product from wild-type and targeted alleles, every reaction will result in a product and thus acts as a control on the other reaction. The dark bar represents the targeted exon with the restriction site (*SfiI*) into which the targeting vector (grey bar under 'targeted allele') was inserted. Each animal was genotyped using two reactions, as shown in *B*. Reaction 1 contained primers 1, 2 and 3; Reaction 2 contained primers 1, 3 and 4.

Figure 8

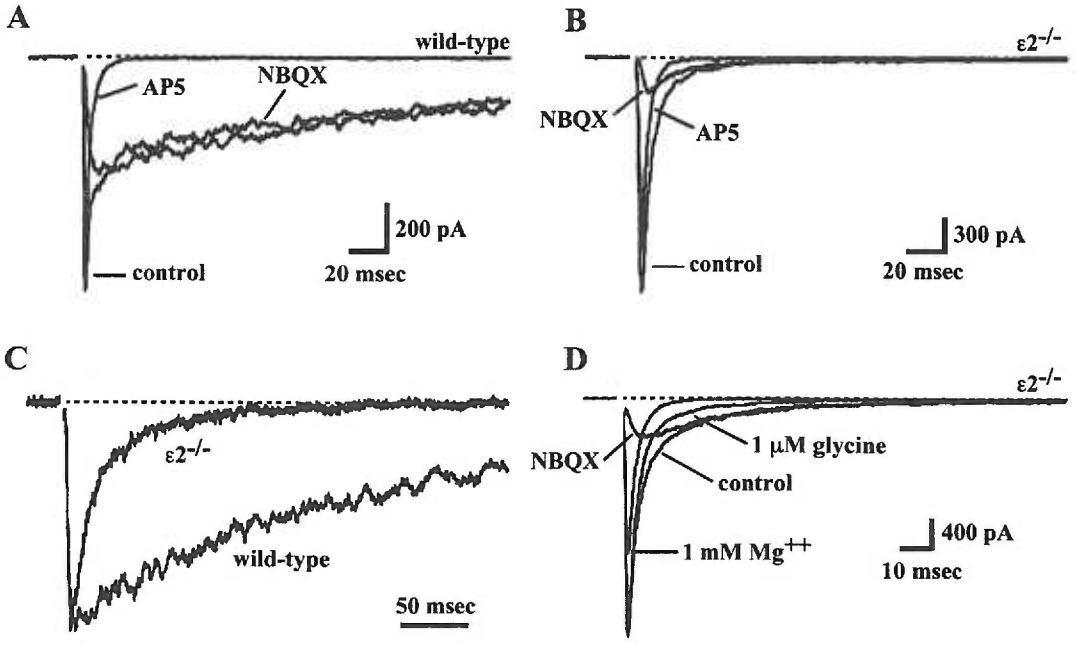
A
wild-type
AP5
NBQX
200 pA
control
20 msec
B
ε2-/-
NBQX
AP5
300 pA
control
20 msec
C
ε2-/-
wild-type
50 msec
D
ε2-/-
NBQX
1 μM glycine
control
1 mM Mg++
400 pA
10 msec

Figure 8.

Fast kinetics of NMDA receptor-mediated EPSCs in $\varepsilon 2^{-/-}$ hippocampal neurons. EPSCs in wild-type (*A*) and $\varepsilon 2^{-/-}$ (*B*) neurons show both NBQX- and AP5-sensitive currents. The AP5-sensitive currents are superimposed and normalized in *C* , showing that the deactivation kinetics of the AP5-sensitive current in *B* were much faster than the AP5-sensitive current in *A*. In *D*, the slow component of the EPSC is decreased by lowering the glycine concentration and completely blocked by 1 mM Mg^{++} (NBQX-sensitive current is shown), characteristic of NMDA channels. The control, NBQX and 1 mM Mg^{++} currents were done in 10 μM glycine.

Figure 9

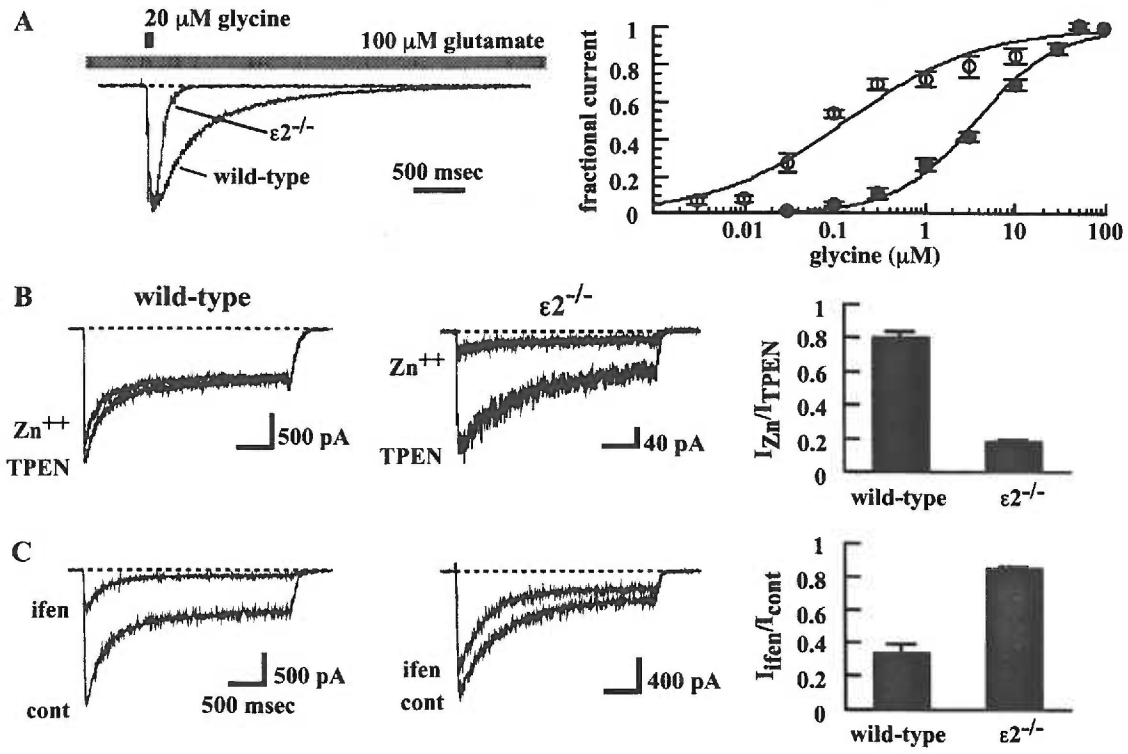
A
20 μM glycine
100 μM glutamate
ε2-/-
wild-type
500 msec
fractional current
1
0.8
0.6
0.4
0.2
0
0.01
0.1
1
10
100
glycine (μM)
B
wild-type
ε2-/-
Zn++
TPEN
500 pA
40 pA
IZn/ITPEN
wild-type
ε2-/-
C
ifen
cont
500 pA
500 msec
400 pA
Iifen/Icont
wild-type
ε2-/-

Figure 9.

The pharmacological characteristics of NMDA receptors from $\varepsilon 2^{-/-}$ neurons are consistent with $\zeta 1/\varepsilon 1$ receptors. *A* (left), The deactivation time course of glycine-activated currents (20 μM, 100 msec) in the continuous presence of glutamate (100 μM) was much faster in neurons lacking $\varepsilon 2^{-/-}$, consistent with a faster microscopic dissociation rate. Glycine deactivation kinetics were measured using calibration-grade glutamate. *A* (right) Steady-state glycine dose-response curve for wild-type (open circles) and $\varepsilon 2^{-/-}$ (closed circles) neurons to NMDA applications. All responses were normalized to the response at 50 μM (wild-type) or 100 μM ($\varepsilon 2^{-/-}$). From the logistic equation, the EC50 was 0.133 μM (wild-type) and 3.61 μM ($\varepsilon 2^{-/-}$) with Hill coefficients of 0.80 (wild-type) and 0.97 ($\varepsilon 2^{-/-}$). NMDA receptors from $\varepsilon 2^{-/-}$ neurons were blocked by low concentrations of Zn^{++} but much less sensitive to ifenprodil. *B*, Wild-type (left) and $\varepsilon 2^{-/-}$ currents (center) in the presence of 500 nM added Zn^{++} or the high-affinity Zn^{++} chelator TPEN. *C*, Compared to wild-type currents (left), currents from $\varepsilon 2^{-/-}$ neurons (center) were much less sensitive to ifenprodil (3 μM).

Figure 10

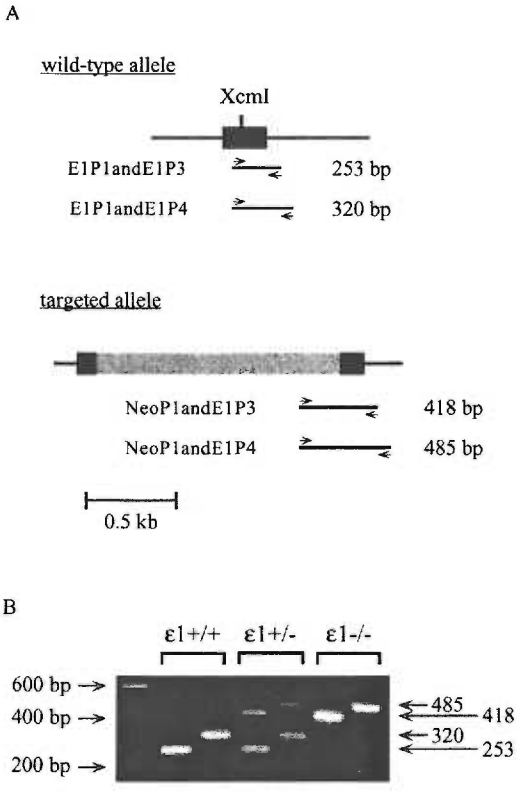
A
wild-type allele
XcmI
E1P1andE1P3
253 bp
E1P1andE1P4
320 bp
targeted allele
NeoP1andE1P3
418 bp
NeoP1andE1P4
485 bp
0.5 kb
B
ε1+/+
ε1+/-
ε1-/-
600 bp
400 bp
200 bp
485
418
320
253

Figure 10.

Genotyping of ε1-targeted mice.

A shows the structure of the the wild-type and ε1-targeted allele. The small arrows indicate alignment of the PCR primers with the genomic DNA. The targeted exon is represented by a thick black line while the targeting vector is represented by the gray bar. Thin lines represent intronic DNA. *B* shows the result of genotyping three different mice. Each mouse is represented by two lanes. The center two lanes shows the predicted products for an animal heterozygous at the ε1 allele. The pairs of bands flanking the center bands indicate only the products expected from wild-type animals (left) or products expected from $\varepsilon 1^{-/-}$ animals (right).

Figure 11

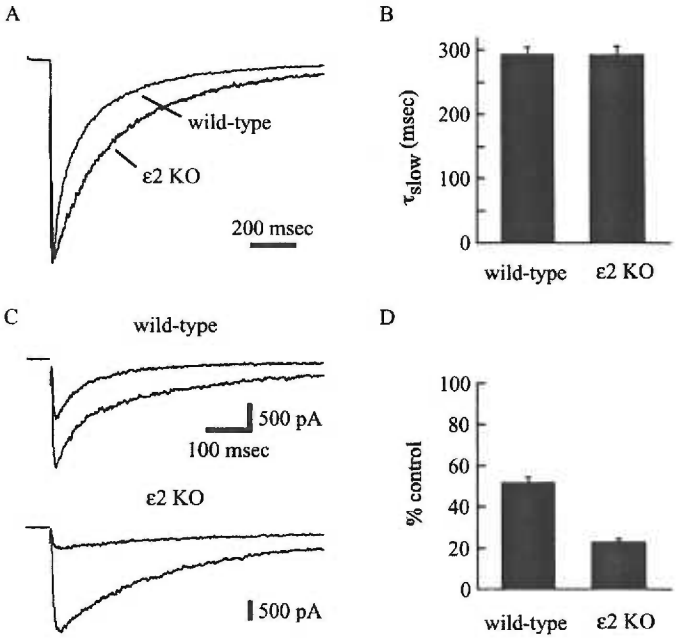
A
wild-type
ε2 KO
200 msec
B
300
200
100
0
τ_{slow} (msec)
wild-type
ε2 KO
C
wild-type
500 pA
100 msec
ε2 KO
500 pA
D
100
80
60
40
20
0
% control
wild-type
ε2 KO

Figure 11.

Excitatory postsynaptic currents from neurons lacking the ε1 subunit.

A,shows evoked EPSCs from wild-type and $\varepsilon 2^{-/-}$ neurons. Currents were normalized. EPSCs from $\varepsilon 2^{-/-}$ neurons were significantly slower than wild-type currents. This resulted from the presence of τ_{fast} in wild-type EPSCs because τ_{slow} was identical between wild-type and $\varepsilon 1^{-/-}$ neurons (*B*). Figures *C* and *D* show comparisons of the ifenprodil sensitivity of wild-type and $\varepsilon 1^{-/-}$ neurons. Wild-type neurons were significantly less sensitive to the ε2-selective antagonist ifenprodil.

Figure 12

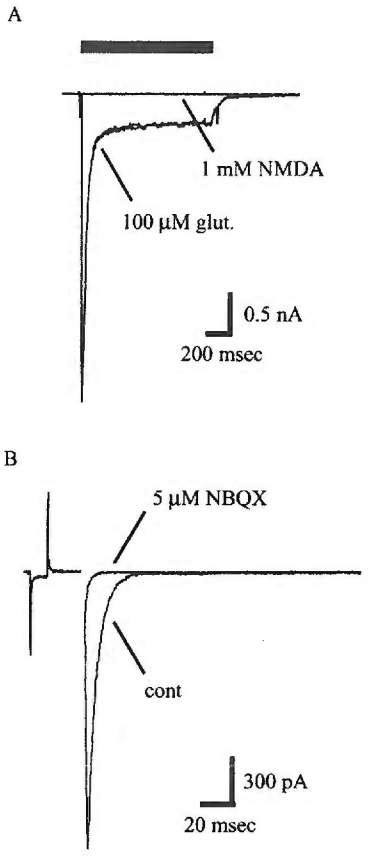
A
1 mM NMDA
100 µM glut.
0.5 nA
200 msec
B
5 µM NBQX
cont
300 pA
20 msec

Figure 12.

Neurons lacking the ε1 and ε2 subunits lack NMDA receptors.

A, No current resulted from the application of NMDA (1 mM; 1 sec) whereas glutamate application (100 μM) resulted in an inward current, presumably resulting from AMPA receptor activation. *B*, NMDA receptor-mediated EPSCs were absent from neurons lacking ε1 and ε2. Synapses formed normally, as determined by the presence of the AMPA receptor-mediated EPSC. Stimulus artifact was removed for clarity.

Figure 13

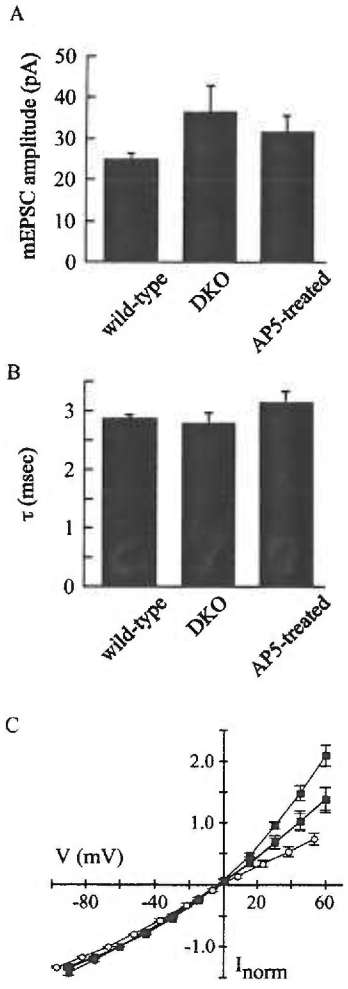
A
mEPSC amplitude (pA)
50
40
30
20
10
0
wild-type
DKO
AP5-treated
B
τ (msec)
3
2
1
0
wild-type
DKO
AP5-treated
C
2.0
1.0
V (mV)
-80
-40
20
60
-1.0
Inorm

Figure 13.

AMPA receptors in ε1-/- ε2+/- neurons.

A, The mean miniature excitatory postsynaptic current amplitudes were not different between wild-type, e1-/- e2-/- neurons, or neurons cultured in the NMDA receptor antagonist AP5 (200 μM). *B*, Similarly, the deactivation time constants were also not different. The current/voltage relationship (*C*), however, showed differences in the rectification properties between wild-type neurons (squares) and $\varepsilon 1^{-/-}$ $\varepsilon 2^{-/-}$ neurons(circles). The presence of spermine (1 mM) in the recording pipette (indicated by the filled symbols) increased the rectification in both cases. Currents were measured at steady-state amplitudes. To facilitate comparisons, all currents were normalize to the current at -60 mV or -67 mV.

Figure 14

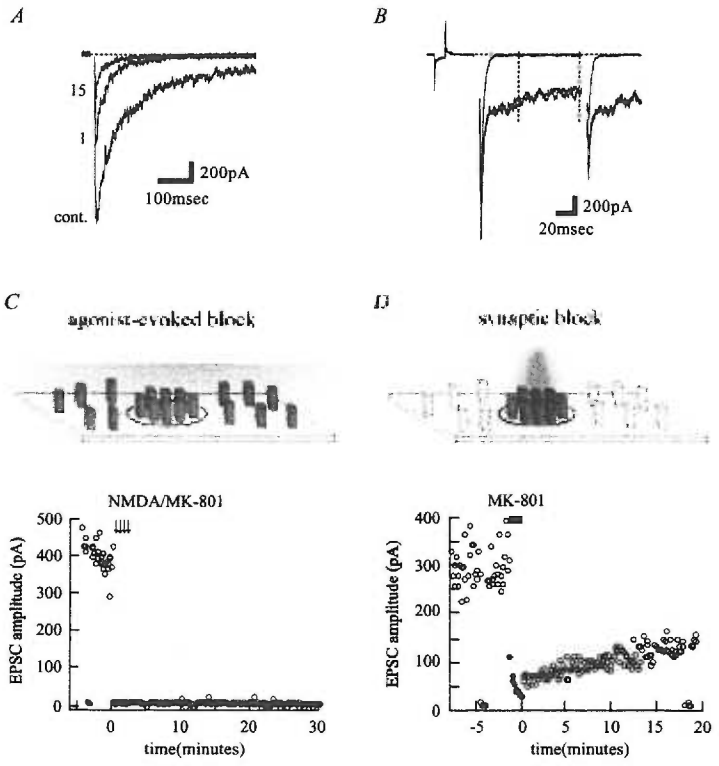
A
15
1
cont.
200pA
100msec
B
200pA
20msec
C
agonist-evoked block
D
synaptic block
NMDA/MK-801
EPSC amplitude (pA)
time(minutes)
MK-801
EPSC amplitude (pA)
time(minutes)

Figure 14.

Anomalous recovery of NMDA receptor-mediated EPSCs following MK-801 block.
(*A*) MK-801 progressively blocked the NMDA receptor-mediated EPSC and accelerated the deactivation. EPSCs before MK-801 ('cont.') and after 1 and 15 stimuli in MK-801 are shown.

(*B*) Paired pulse stimuli evoked EPSCs (100 msec interpulse interval) with both AMPA and NMDA components. For these experiments, NMDA-receptor mediated EPSCs were averaged between the parallel dashed lines, well after the decay of the AMPA component. Stimulus artifacts were blanked.

(*C*) Agonist-evoked block of synaptic receptors is shown in (*C*). Whole-cell application (3 X 1 sec) of NMDA (1 mM) in the presence of MK-801 (20 μM) resulted in complete and irreversible block of the NMDA receptor-mediated EPSC. Each point represents a paired-pulse episode.

(*D*) Selective block of synaptic NMDA receptors by application of MK-801 (5-20 μM) also completely blocked the EPSC. However following removal of MK-801, the EPSC showed a 30% recovery over the course of several minutes. Filled circles indicate MK-801 application.

Figure 15

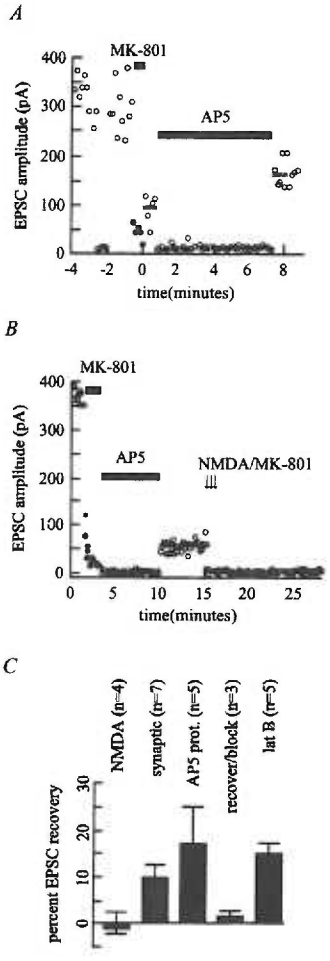
A
MK-801
AP5
EPSC amplitude (pA)
400
300
200
100
0
-4
-2
0
2
4
6
8
time(minutes)
B
MK-801
AP5
NMDA/MK-801
EPSC amplitude (pA)
400
300
200
100
0
0
5
10
15
20
25
time(minutes)
C
NMDA (n=4)
synaptic (n=7)
AP5 prot. (n=5)
recover/block (n=3)
lat B (n=5)
percent EPSC recovery
30
20
10
0

Figure 15.

The recovery of EPSC following irreversible block of synaptic NMDA receptors by MK-801 suggests the appearance of new receptors at the synapse.

(*A*) The NMDA receptor antagonist DL-AP5 did not prevent recovery of the EPSC, suggesting that recovery was not due to MK-801 unbinding following evoked release of glutamate. Following removal of MK-801 (10 μM), the average EPSC amplitude (gray bars) was measured before and following 50 EPSCs in the continuous presence of the competitive antagonist DL-AP5 (200 μM). The recovery after 50 stimuli was not different from recovery in the absence of DL-AP5.

(*B*) The NMDA receptors underlying the recovery of the EPSC were irreversibly blocked by whole-cell co-application of NMDA and MK-801, indicating that receptors with lower affinity for MK-801 did not account for the recovery.

(*C*) Fractional recovery of EPSC following whole-cell NMDA application ('NMDA'), synaptic stimulation ('synaptic'), post-block application of AP5 ('AP5 prot.'), whole-cell application NMDA application to recovered EPSC ('recover/block') and latrunculin treatment ('Lat B').

Figure 16

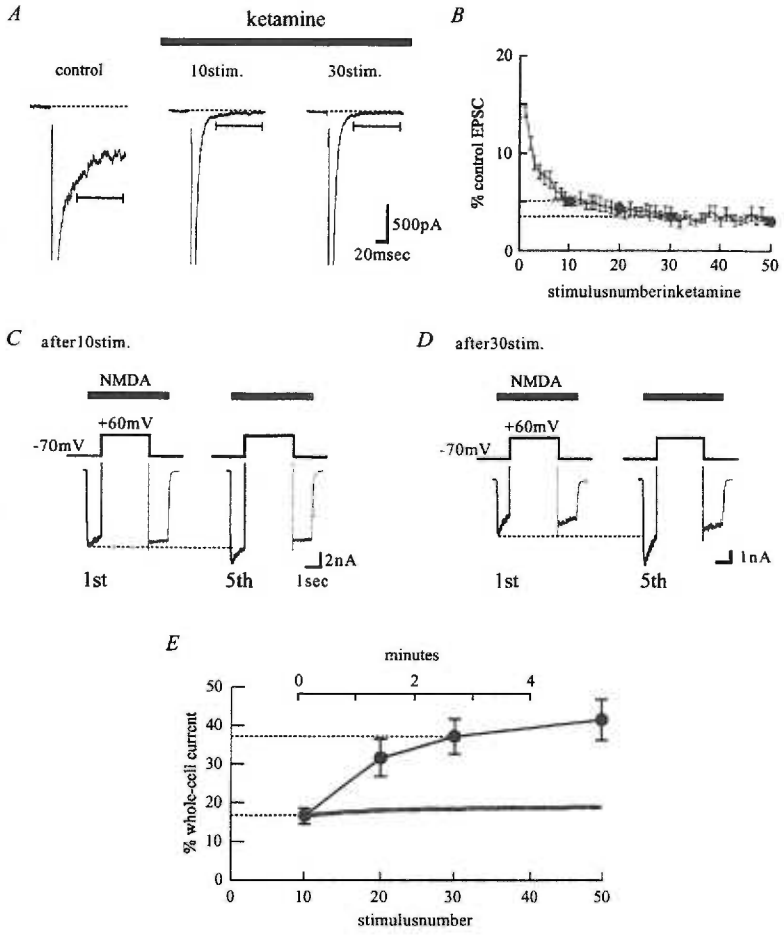
A
ketamine
control
10stim.
30stim.
500pA
20msec
B
% control EPSC
stimulusnumberinketamine
C after10stim.
NMDA
+60mV
-70mV
2nA
1st
5th
1sec
D after30stim.
NMDA
+60mV
-70mV
1nA
1st
5th
E
minutes
% whole-cell current
stimulusnumber

Figure 16.

NMDA receptors are continually moving into the synapse.

(A,B) Bath application of ketamine largely blocked the NMDA receptor-mediated EPSC (measured over bracketed segment) after 10 stimuli without affecting the AMPA component. The progressive block of the EPSC in ketamine (**B**) indicates that only a slight additional block of the NMDA receptor-mediated EPSC was measurable after 30 stimuli. By stimulus 10, 5.08±0.46% of the EPSC remained compared to 3.48±0.94% at 30 stimuli.

(C,D) To determine the fraction of NMDA receptors on the entire cell that were blocked by ketamine during synaptic stimulation, we examined whole-currents evoked by 5 sec applications of NMDA (100 μM, solid bars) immediately following either 10 or 30 synaptic stimulations in ketamine. A 3 sec depolarization to +60 mV was delivered in the middle of the agonist application to relieve ketamine block of synaptic receptors. The first and final of a series of 5 NMDA applications are shown. After 10 synaptic stimuli, the NMDA current after 4 depolarizations had increased, representing the population of synaptic receptors that had been blocked with ketamine (*C*). After 30 synaptic stimuli, the number of receptors unblocked by the depolarizations was much larger (*D*). Outward currents during the depolarization were blanked; the inward current following the depolarization (shown in light traces) was not used to measure ketamine unblock due to contamination by NMDA receptor desensitization and tail currents from voltage-gated conductances. The percent whole-cell current blocked by ketamine was calculated as [1-(inward current of the first application/peak inward current of final application)].

(E) The fraction of blocked synaptic receptors, taken from data in part B, changed very little between 10 and 50 synaptic stimuli (solid gray line). However, the fraction of the receptors on the entire cell that was unblocked with the protocol show in C and D was strongly dependent on the number of synaptic stimuli (black circles). This is inconsistent with a fixed population of synaptic receptors. Specifically, between 10 and 50 synaptic stimuli, the number of 'synaptic' receptors

had increased from ~17% to ~42% of the receptors on the cell, consistent with movement of receptors into the synapse.

Figure 17

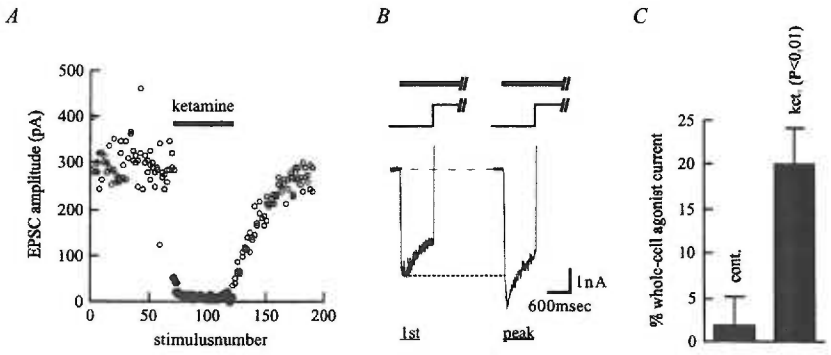
A
B
C
EPSC amplitude (pA)
500
400
300
200
100
0
ketamine
0
50
100
150
200
stimulusnumber
1nA
600msec
1st
peak
% whole-cell agonist current
25
20
15
10
5
0
cont.
ket. (P<0.01)

Figure 17.

NMDA receptors move out of the synapse.

(A,B) Synaptic NMDA receptors were blocked by ketamine during 50 synaptic stimuli, but then subsequently the EPSC recovered to baseline following washout of ketamine (19). The mean amplitude of the recovered EPSCs was 101.9±0.04% of control (n=6) indicating that ketamine-bound receptors were no longer part of the synaptic complement. However, as shown in Figure B, the ketamine unblocking protocol as used in Figure 2 revealed that there was a significant number of previously synaptic receptors that were still blocked by ketamine. Dark bars indicate NMDA (100 μM) applications. Only the inward current before the depolarization is shown. Filled circles indicate ketamine application.

(C) The number of previously synaptic receptors constituted 20.02±4.3% of the whole-cell current for EPSCs treated with ketamine. The ketamine unblock protocol did not unmask any additional receptors in neurons that were not treated with ketamine. These results suggest that ketamine-bound receptors had moved from synaptic to extrasynaptic regions.

Figure 18

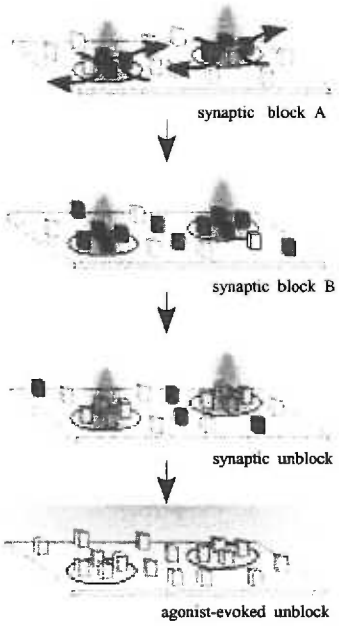
synaptic block A
synaptic block B
synaptic unblock
agonist-evoked unblock

Figure 18.

Schematic of movement of NMDA receptors in and out of the synapse. Darkened boxes represent receptors that are blocked by channel blocker. Circle represents the area where NMDA receptors can bind to synaptically-released glutamate. See text for explanation.